Atmos. Chem. Phys. Discuss., 14, 19095–19147, 2014
www.atmos-chem-phys-discuss.net/14/19095/2014/
doi:10.5194/acpd-14-19095-2014

Atmospheric Chemistry and Physics Discussions

A multi-model evaluation of aerosols over South Asia: Common problems and possible causes

X. Pan[1], M. Chin[1], R. Gautam[1,2], H. Bian[1,3], D. Kim[1,2], P. R. Colarco[1], T. L. Diehl[1,2,*], T. Takemura[4], L. Pozzoli[5], K. Tsigaridis[6,7], S. Bauer[6,7], and N. Bellouin[8]

[1]NASA Goddard Space Flight Center, Greenbelt, MD, USA
[2]Universities Space Research Association, Columbia, MD, USA
[3]University of Maryland Baltimore City, Baltimore, MD, USA
[4]Kyushu University, Fukuoka, Japan
[5]Istanbul Technical University, Istanbul, Turkey
[6]NASA, Goddard Institute for Space Studies, New York, NY, USA
[7]Center for Climate Systems Research, Columbia University, New York, NY, USA
[8]Department of Meteorology, University of Reading, Reading, Berkshire, UK
[*]now at: European Commission at the Joint Research Center, Ispra, Italy

Received: 6 June 2014 – Accepted: 3 July 2014 – Published: 22 July 2014

Correspondence to: X. Pan (xiaohua.pan@nasa.gov)

Published by Copernicus Publications on behalf of the European Geosciences Union.

Abstract

Atmospheric pollution over South Asia attracts special attention due to its effects on regional climate, the water cycle, and human health. These effects are potentially growing owing to rising trends of anthropogenic aerosol emissions found there. In this study, the spatio-temporal aerosol distributions over South Asia from 7 global models, for the period of 2000–2007, are evaluated systematically against aerosol retrievals of NASA satellite sensors and ground-based measurements. Overall, substantial underestimations of aerosol loading over South Asia are found systematically in 6 out of 7 models. Averaged over the entire South Asia, the annual mean Aerosol Optical Depth (AOD) is underestimated by a range of 18–45 % across models compared to MISR, which is the lowest bound among various satellite AOD retrievals (from MISR, SeaWiFS, MODIS Aqua and Terra). In particular at Kanpur located in northern India, AOD is underestimated even more by a factor of 4, and annual mean Aerosol Absorption Optical Depth (AAOD) is underestimated by about a factor of 2 in comparison with AERONET, during the post-monsoon and the wintertime periods (i.e. October–January) when agricultural waste burning and anthropogenic emissions dominate. The largest model underestimation of aerosol loading occurs in the lowest boundary layer (from surface to 2 km) based on the comparisons with aerosol extinction vertical distribution from CALIPSO. The possible causes for the common problems of model aerosol underestimation over south Asia are identified here, which are suggested as the following. During the winter, not only the columnar aerosol loading in models, but also surface concentrations of all aerosol components (sulfate, nitrate, organic aerosol and black carbon) are found lower than observations (ISRO-GBP, ICARB and CALIPSO), indicating that anthropogenic emissions, especially biofuel, are likely underestimated in this season. Nitrate, a major component of aerosols in South Asia, is either not considered in 4 out of 7 models or significantly lower than observations in other 2 models. Surprisingly, the near-surface relative humidity in these models is found significantly lower than observations in the winter, resulting in suppression of the hygroscopic growth of soluble

ACPD
14, 19095–19147, 2014

aerosols and formations of sulfate and nitrate, and thereby underestimation of AOD. During the post-monsoon season, the deficiency of agricultural waste burning emissions in GFED2 biomass burning emission inventory, used by the models, partly contributes to the model underestimation of aerosol loading over South Asia in burning seasons.

1 Introduction

South Asia (Fig. 1), particularly the Indo-Gangetic Plain (IGP) in northern India, is one of the global hotspots with high aerosol optical depth (AOD) routinely observed from satellite remote sensing observations (e.g. from Moderate Resolution Imaging Spectroradiometer or MODIS, Multi-angle Imaging SpectroRadiometer or MISR and Sea-Viewing Wide Field-of-View Sensor or SeaWiFS), as well as from ground-based measurements (e.g. Aerosol Robotic Network or AERONET). The potential influence of absorbing aerosols on the South Asian climate and water cycle (e.g. Indian summer monsoon) via surface dimming and atmospheric warming is also widely discussed in the literature (e.g. Ramanathan et al., 2005; Lau et al., 2006). In addition, recent studies have showed that large concentrations of absorbing aerosols, such as dust and black carbon (BC), over the IGP and Himalayan foothills are linked to snow albedo reduction and accelerated snow/ice melt in the Himalaya during the pre-monsoon season (Lau et al., 2010; Qian et al., 2011; Yasunari et al., 2010; Gautam et al., 2013). BC surface concentrations in northern India have been reported to be much higher than in other world regions and mega cities (Tripathi et al., 2005; Ganguly et al., 2006), and the atmospheric heating due to aerosols (mainly BC) is estimated to be large, about 50–70 $W\,m^{-2}$, especially during the wintertime (Ganguly et al., 2006).

Besides these climate impacts, fine aerosol particles ($PM_{2.5}$ – particulate matter less than 2.5 µm in diameter) are known to affect public health, especially over the IGP region where large portions of the Indian population live. At Delhi, for example, the annual mean $PM_{2.5}$ concentration in 2007 was about $97 \pm 56\,\mu g\,m^{-3}$ (Tiwari et al., 2009), nine

ACPD
14, 19095–19147, 2014

times the 2005 air quality guidelines recommended by the World Health Organization (WHO).

Increases in anthropogenic aerosol emissions and loading in South Asia in recent decades have been well documented (Ohara et al., 2007; Hsu et al., 2012; Kaskaoutis et al., 2012; Babu et al., 2013), contrasting with decreasing trends emissions over Europe and North America (Hsu et al., 2012; Chin et al., 2014).

It is undoubted that the study of interaction of aerosol and climate as mentioned aboved as well as performances of aerosol forecast and future climate projections depend on the reliability of the model simulations of the past and current climate. Therefore, it is critical to accurately represent aerosol sources, distributions and properties in climate models over this heavily polluted region, South Asia. Previous studies, however, reported that global models underestimated the AOD over South Asia, especially over the IGP in the winter (Dickerson et al., 2002; Reddy et al., 2004; Chin et al., 2009; Ganguly et al., 2009; Henriksson et al., 2011; Goto et al., 2011; Cherian et al., 2013; Sanap et al., 2014). Among them, Ganguly et al. (2009) reported that the GFDL-AM2 model largely underestimated the AOD over the IGP during the winter by about a factor of 6. Recently, the AOD simulated by the regional climate model (RegCM4) showed a good agreement with the observed AOD from AERONET over dust-dominated areas in south Asia, but AOD was underestimated over regions that are impacted by anthropogenic emission (Nair et al., 2012). In terms of aerosol vertical distribution over South Asia, 11 of the 12 models participating in the AeroCom phase I model intercomparison were also found to underestimate the aerosol vertical extinction over South Asia, especially under 2 km, in comparison with the space-borne lidar measurements from the Cloud-Aerosol Lidar and Infrared Pathfinder Satellite Observations (CALIPSO) satellite (Koffi et al., 2012). The ability to capture surface BC concentrations over South Asia for models has been found similarly limited. The low biases tend to be larger in the winter (Ganguly et al., 2009; Menon et al., 2010; Nair et al., 2012; Moorthy et al., 2013). These studies have revealed the challenges for models to adequately represent the aerosol loading over South Asia.

ACPD
14, 19095–19147, 2014

Extending from previous studies and utilizing the recent model outputs from the Aerosol Comparisons between Observations and Models (AeroCom) Phase II multi-model experiments, the present work systematically evaluates global model simulations of aerosols in South Asia with observations from satellites and ground-based measurements, and strives to characterize the causes for the model deficiency in reproducing observations. The outcomes of this study will help us understand the discrepancies between models and observations, thus providing directions for future model improvements in this important region of South Asia.

The description of models is given in Sect. 2. The observation data from satellites and ground-based measurements are introduced in Sect. 3. We present the results in Sect. 4, including the comparisons of the multi-model simulations with observations in terms of horizontal, vertical and temporal distribution of AOD (and aerosol absorption optical depth, or AAOD when available), and the surface BC concentration. The possible causes for the underestimations of aerosol load found in models are investigated in Sect. 5. Major findings are summarized in Sect. 6.

2 Model description

2.1 Models

The aerosol simulations for the period of 2000–2007 from 7 models, including 6 models that participated in AeroCom Phase II hindcast experiment (i.e. AeroCom II HCA) and one additional model, GEOS5, are analyzed in this paper (see Table 1 for details). Given that MODIS-Terra is available only after 2000, we chose the years 2000–2007 in this study, although longer time period of simulations (starting from 1980) are available from the six AeroCom models (note that ECHAM5-HAMMOZ ended in 2005 and HadGEM2 in 2006). GEOS5 is similar to GOCART because its aerosol module is developed from GOCART but with modifications (Colarco et al., 2010). More detailed descriptions about these models can be found in previous studies (see references

ACPD
14, 19095–19147, 2014

listed in Table 1 and Myhre et al., 2013). All models include sulfate (SO_4^{2-}), BC, organic aerosol (OA), dust (DU) and sea salt (SS). Nitrate (NO_3^-) is included in only 3 models (GISS-modelE, GISS-MATRIX and HadGEM2). The secondary organic aerosol (SOA) chemistry is resolved only in 2 models, i.e. GISS-modelE and HadGEM2 (offline scheme in this model), and simple estimations of SOA are included in the remaining models. Among the 7 models, aerosol optical properties are treated differently although all optical properties are derived from Mie theory. In order to compare closely with the measurements from satellites and AERONET, clear-sky AODs of the two GISS models are used in this study, which is not available in other 5 models (only all-sky AOD is available). All 7 models use the assimilated wind fields, although from different assimilation datasets. The horizontal resolutions vary from 2.8° by 2.8° (ECHAM5-HAMMOZ) to about 1.1° by 1.1° (SPRINTARS) and the vertical levels range from 30 (GOCART-v4) to 72 (GEOS5). More information is given in Table 1.

2.2 Emissions

For anthropogenic emissions, which are mainly from consumption of fossil fuel and biofuel, the models choose either A2-ACCMIP or A2-MAP emission dataset. Both A2-MAP and A2-ACCMIP were constructed by combining multiple inventories but in different ways. The anthropogenic emissions from A2-MAP have inter-annual variability based on reported activity data, while those from A2-ACCMIP do not because they are generated via linear interpolation between decadal endpoints. Over South Asia, the spatial distribution and total emission amount are different between these two emission datasets, with higher emission amount in A2-ACCMIP. Detailed information on these two emission datasets can be found in Diehl et al. (2012).

Figure 2 shows the averaged annual mean (2000–2007) anthropogenic BC, OA, SO_2, NH_3 and NO_x emissions from A2-ACCMIP anthropogenic emission dataset (A2-MAP is not shown and it does not provide NH_3 and NO_x emissions). Note that the seasonal cycle of anthropogenic emission is not resolved in either emission dataset,

ACPD
14, 19095–19147, 2014

which could be problematic especially for biofuel emission in this region (discussed in Sect. 5.2). The anthropogenic emissions display high spatial heterogeneities over South Asia, coinciding with those of the population distribution as reported by multiple previous studies (e.g. Girolamo et al., 2004). Densely populated regions are usually associated with heavy anthropogenic emissions in south Asia, such as the IGP region in northern India (as indicated in Fig. 1). In A2-ACCMIP (A2-MAP), the anthropogenic emission from SO_2 is about 7.426 (5.279) Tg SO_2 yr^{-1}, NH_3 about 4.934 Tg NH_3 yr^{-1}, NO_x is about 4.330 Tg NO_x yr^{-1}, Organic aerosol (OA) about 3.455 (2.678) Tg C yr^{-1}, and BC about 0.681 (0.633) Tg C yr^{-1} in South Asia (refer to Fig. 2).

Open biomass burning, including the agricultural residue burned in the field and forest burning, also contribute significantly to the total aerosol loading over India, about 25 % of BC and OC (Venkataraman et al., 2006). Figure 3 shows the seasonal BC biomass burning emission based on monthly Global Fire Emissions Database Version 2 (GFED2), from which the biomass burning emissions in A2-ACCMIP and A2-MAP emissions inventories are derived. OA and SO_2 show similar spatial patterns and proportional amounts as BC (not shown here). The open biomass burning displays strong geographical and seasonal variations. Pre-monsoon period is the most active open biomass burning season with an emission amount of 0.118 Tg C yr^{-1} over South Asia, especially concentrated over northeastern India associated with the Jhum cultivation to clear the forest and create fields (Vadrevu et al., 2013). Seasonal practices of biomass burning from agricultural crop residues associated with rice-wheat crop rotation system over the western IGP, such as Punjab, Haryana and western Uttar Pradesh, could explain the high aerosol loading during the post-monsoon season (Badarinath et al., 2009a; Sharma et al., 2010; Vadrevu et al., 2011, 2013) with a total emission amount of 0.011 Tg C yr^{-1} over the entire South Asia.

The major natural aerosol over South Asia is the wind-blown mineral dust from the arid and semi-arid regions of southwest Asia, such as Iran, Afghanistan, Pakistan, Arabian Peninsula, and Thar Desert in the northwestern India. The dust emissions among the model simulations are quite diverse, which vary from 11.7 ± 4.2 (ECH) to

ACPD
14, 19095–19147, 2014

157.4 ± 28.8 (SPR) Tg yr^{-1} (averaged for 2000–2007 over South Asia). This model diversity is attributed to differences in the model size range of the emitted particles, parameterization of source strength, and wind fields and soil properties over source regions. Since this specified region mainly consists of land areas, the sea salt emission is negligible.

3 Observation dataset

3.1 Satellite data

In this study, five satellite data products are used to characterize aerosol distribution and evaluate the model simulations. Level 3 monthly AOD from MODIS Terra and Aqua Collection 5.1 were produced by averaging the daily aerosol products at $1^{\circ} \times 1^{\circ}$ grid. The MODIS AOD (at 550 nm), shown in this study, is a composite of the Dark Target (Levy et al., 2010) and Deep Blue retrieval products (Hsu et al., 2006), as the latter is able to retrieve AOD over bright surfaces such as the Thar Desert. The SeaWiFS aerosol retrieval combined the Deep Blue algorithm over land (Hsu et al., 2006, 2012) and Ocean Aerosol Retrieval (SOAR) algorithm over ocean (Sayer et al., 2012). MISR (at 555 nm) retrieves aerosol properties over a variety of terrain, including bright surface like deserts, which is attributed to its unique multi-angle capability (Martonchik et al., 2004; Kahn et al., 2007). Since South Asia is covered by frequent cloudiness during the summer monsoon season (June to September), the quality of monthly mean AOD during this season is likely to be affected by the low sample size.

We also use the vertical extinction profiles from the Cloud-Aerosol Lidar with Orthogonal Polarization (CALIOP) onboard the satellite CALIPSO layer product version 3.01 (climatology of June 2006–December 2011) to evaluate the model simulated aerosol vertical distribution in 2006 (Koffi et al., 2012). Only the CALIOP observations in 532 nm channel and nighttime are used because of their better signal-to-noise than the 1064 nm and daytime observations. Three parameters are applied to facilitate this

ACPD
14, 19095–19147, 2014

evaluation, namely AOD, Z_a (km) and F_{2km} (%). AOD is the integral of extinction coefficient within the entire column (Eq. 1). Z_a is defined as the averaged aerosol layer height (Eq. 2). F_{2km} is defined as the percentage of AOD located in the lowest 2 km (Eq. 3) in the column.

$$\mathrm{AOD} = \sum_{i=1}^{n} \mathrm{EXT}_i \times \Delta Z_i \tag{1}$$

$$Z_a = \frac{\sum_{i=1}^{n} \mathrm{EXT}_i \times Z_i}{\sum_{i=1}^{n} \mathrm{EXT}_i} \tag{2}$$

$$F_{2km} = \frac{\sum_{i=1}^{\text{level of 2 km}} \mathrm{EXT}_i \times \Delta Z_i}{\sum_{i=1}^{n} \mathrm{EXT}_i \times \Delta Z_i} \tag{3}$$

Where, EXT_i is the extinction coefficient at i level (i = 1 to n, i.e. from the lowest 100 m to the top of atmosphere), Z_i is altitude (km) of level i and ΔZ_i is the depth of level i.

3.2 AERONET

In this study, we use AOD and AAOD data from the ground-based AERONET (Holben et al., 1998) sites in South Asia. Monthly mean AOD and AAOD at 500 nm were analyzed over Kanpur, Lahore and Karachi. Here, version 2 Level 2 data were used, which are cloud-screened and quality-assured. Locations of these three stations are shown in Fig. 1 along with 11 in-situ measurement sites as described in the following Sect. 3.3. The information of all 14 ground-based measurement sites is given in Table 2.

ACPD
14, 19095–19147, 2014

3.3 In-situ measurements

We evaluate the modeled BC concentrations with the surface in-situ measurements from the Integrated Campaign for Aerosols gases and Radiation Budget (ICARB) field campaign in India over 8 stations, which spread over Indian mainland and islands for the entire year of 2006. The measured ICARB BC data is recorded from inter-compared aethalometers following a common protocol. More details of ICARB can be found in previous publications (e.g. Beegum et al., 2009 and Moorthy et al., 2013).

In order to examine the chemical composition (such as surface concentrations of nitrate, sulfate, organic aerosol and black carbon) and meteorological conditions (such as surface relative humidity and temperature) of winter haze over IGP in multi-models, we refer to the measurements from the Indian Space Research Organization Geosphere Biosphere Programme (ISRO-GBP) which provided valuable information about aerosol physical, optical and chemical properties along the IGP during wintertime (i.e. December 2004/January 2005). In this study, 4 stations in IGP are selected because of their relatively complete measurements, i.e. Hisar (Ramachandran et al., 2006; Rengarajan et al., 2007; Das et al., 2008), Agra (Safai et al., 2008), Kanpur (Tripathi et al., 2006; Tare et al., 2006) and Allahabad (Ram et al., 2012).

4 Results

In this section, the aerosol simulations by multi-models are evaluated in comparison to satellite data and ground-based measurements in terms of temporal variation and spatial distribution (horizontally and vertically) over South Asia.

4.1 Interannual variability of AOD

Figure 4a shows the annual averaged mean AOD over the entire South Asia domain (denoted by green shaded area) for the period of 2000–2007. The AOD is 0.281 and 0.282 from MISR and SeaWiFS (SeaW) retrievals respectively, and 0.348 and 0.355

ACPD
14, 19095–19147, 2014

from MODIS Aqua (MODIS-a) and Terra (MODIS-t) respectively. Six out of seven models (except for HAD) consistently underestimated AOD by 0.052–.126 or 18–45 %, compared to MISR, the lowest bound of four satellite retrievals. As shown in Fig. 4b, over the central IGP region (77–83° E/25–28° N, denoted by the white box in Fig. 4a) where the hotspot of AOD is observed from satellites, the performance of the same six models are even worse, with the annual averaged mean AOD underestimated by 20–56 % relative to MISR. Unlike other models, HAD shows a comparable AOD with MISR and SeaWiFS over the entire South Asia, and exceeds all satellite data over the central IGP. As shown in Fig. 4a, the peak AOD in 2003 and the low AOD in 2005 are reflected in all satellites (except MODIS Aqua), which are positively related to the strength of dust emissions during the dry season in that corresponding year (Kaskaoutis et al., 2012; Hsu et al., 2012; Ramachandran et al., 2013). However, all models fail to capture these observed interannual variations of AOD, and only two models (GE5 and SPR) indicate the low AOD in 2005.

4.2 Seasonal cycle of AOD and AAOD over 3 AERONET stations

To further examine the details of underestimations occurring in most models, in this section, monthly variations of AOD and AAOD are compared with the AERONET data at three selected sites in South Asia (Fig. 5). These three locations represent different aerosol environments in South Asia: Kanpur, an industrial city located in the central IGP, is influenced by high anthropogenic emissions throughout the year and by the transported dust during pre-monsoon (MAM) and early monsoon periods (JJA); Lahore, located in the western IGP, is directly influenced by the biomass burning in the pre-monsoon (MAM) and post-monsoon (ON) seasons; and Karachi, an urban coastal city in Pakistan, is influenced by the frequent dust outbreaks, especially from the Arabian peninsula around early summer monsoon season (JJA). A two-year period is chosen for each site, based on the availability of AERONET measurements at that site. The satellite data, namely MODIS-Terra, MISR, and SeaWiFS, are also shown along with AERONET to make an inter-comparison.

ACPD
14, 19095–19147, 2014

At Kanpur (first row of Fig. 5), strong seasonal distribution of AERONET AOD (left column of Fig. 5) are associated with dust outbreaks in May–July, and the active open biomass burning as well as high anthropogenic emissions in October–January. However, only the peak in May–July each year is captured by most models (except HAD) although overestimated in GIM, while the other peak in October–January is largely missing in all models. Different from observations and other models, HAD model simulates AOD with two peaks in April and October, out-of-phase with the observed seasonal cycles. The observed and modeled features mentioned above are repeated almost every year. The discrepancy among models and from AERONET AOD is further diagnosed in the end of this section. As for AAOD (right column of Fig. 5), all models are much lower than the AERONET retrieval by a factor of 2 on average. Although 2 out of 7 models show enhanced AAOD during the dusty period, large underestimation are still pronounced in other models and other seasons when anthropogenic/open biomass burning emissions dominate, implying the underestimation of BC loading or misrepresentation of its optical properties (more analysis on BC in Sect. 4.5).

At Lahore (second row of Fig. 5), AERONET data is available mostly in 2007, when model outputs are available only from five models. Lahore is located in the Punjab region, which is an agriculture region known as the "breadbasket" for the Pakistan and India. The enhanced AERONET AOD and AAOD are evident at Lahore during October–November as shown in Fig. 5, which is linked to the agricultural waste burning after harvest in this area. However, all five models underestimate AOD in each single month, with the largest underestimation found in the October–November (similarly for AAOD). Thereby it suggests that emissions from agriculture waste burning, which is based on GFED2, are likely underestimated in these models (discussed in Sect. 5.3). Compared to observations, HAD again showed abnormal seasonal variation at Lahore as at Kanpur with extreme high AOD in October.

At Karachi (third row of Fig. 5) in 2007, a unimodal distribution is revealed in AERONET AOD, in contrast to the bimodal seasonal variation at Kanpur. The maximum AOD around July is associated with the wind-driven mineral dust from Arabian

ACPD
14, 19095–19147, 2014

Peninsula, which is captured by the models. However, similar to Lahore, all models fail to capture the relative higher AAOD around November, when the open biomass burning is active in the northwestern South Asia (i.e. the area around Lahore) and the smoke is transported southward to the region where Karachi is located (Badarinath et al., 2009a, b).

Overall, in comparison with AERONET and satellite data at the three stations, most models tend to underestimate AOD in October–January when the open biomass burning and anthropogenic emissions are dominant over dust emissions. Regarding the comparison between satellite and AERONET AOD data at these three stations, the monthly variations and amplitudes of all three satellites generally resemble those of AERONET AOD. However, MODIS-Terra is biased high during the pre-monsoon and monsoon months. It is partially because the dark target retrieval in MODIS, which is applied over area like Kanpur, is sensitive to the surface reflectance. The surface reflectance is usually biased low under dusty condition (Jethva et al., 2009), and in turn, the atmospheric contribution, i.e. AOD, is biased high.

In order to diagnose the discrepancies between models and AERONET data, the individual component AOD from only 4 models (HAD, GE5, SPR and GOC, unavailable from other 3 models) are also examined at Kanpur for 2004 in Fig. 6. It is found that the abnormal high peaks in April and October in the HAD model (upper left panel in Fig. 6) are mainly contributed by the nitrate (NO_3^-) AOD, indicating a problem with simulating the seasonal variation and amount of the nitrate aerosol in this model. On the other hand, in December and January, HAD is the only model with the AOD closest to the AERONET data at Kanpur, largely due to nitrate. In fact, nitrate aerosol is expected to be the highest in winter, because high relative humidity and low temperature over IGP in this season favor the formation of NH_4NO_3 (Lewandowska et al., 2004). However, other three models (SPR, GE5 and GOC) do not have the nitrate aerosol component, which may partially explain the underestimations of the peak in the winter (December and January) in these models. In general, based on the results of column AOD from all these four models (i.e. HAD, GE5, SPR and GOC), it is found that the magnitudes and

ACPD
14, 19095–19147, 2014

seasonal cycles of aerosol composition are very different across models, in particular for nitrate, sulfate and dust.

4.3 Spatial distribution of AOD in different seasons

In the previous section, the underestimations of AOD and AAOD are mainly found in October–January based on the model evaluations at three AERONET stations. Here, as shown in Fig. 7a–d, the spatial distributions of AOD over the entire South Asia are compared among 3 satellites, i.e. MODIS-Terra at 550 nm (MODIS-Aqua resembles MODIS-Terra), MISR at 555 nm and SeaWiFS at 550 nm, and 7 models at 550 nm during the winter monsoon (DJF), pre-monsoon (MAM), summer monsoon (JJAS) and post monsoon (ON) phases averaged over 2000–2007. Three aforementioned AERONET stations are also labeled in the spatial maps for reference. In general, the spatial distribution of aerosol is closely associated with the emission source over South Asia, and the aerosol abundance in the atmosphere is modulated by meteorological conditions, such as efficient atmospheric dispersion associated with the prevailing winds in March–July, high wet removal associated with the monsoon rainfall in June–September, and stable atmospheric conditions thus less efficient atmospheric dispersion in December–February.

During the winter season (DJF), local anthropogenic sources dominate over dust, contributing as much as 80 % (± 10 %) to the aerosol loading (Ramanathan et al., 2001). The maximum AOD is found in the central and eastern IGP based on three satellites as shown in Fig. 7a, which coincides with the large SO_2 emissions there (Fig. 2) associated with large thermal power plants (capacity > 1970 MW) (Prasad et al., 2006). The natural topography (i.e. gradually decreased elevation eastward but narrow opening to the Bay of Bengal as shown in Fig. 1) is favorable to the accumulation of aerosol over central and eastern IGP. Additionally, the winter season is characterized by relatively stable atmospheric condition that traps pollutants in the shallow boundary layer, leading to a strengthened hazy condition in the IGP (Girolamo et al., 2004; Gautam et al., 2007). The outflow of aerosols to the Bay of Bengal is well depicted by satel-

ACPD
14, 19095–19147, 2014

lite data. However, only the HAD model captures the observed AOD spatial pattern and amplitude. Other models greatly underestimate the high AOD over IGP region. In addition, the observed north-south gradient of AOD is not captured by most models, with SPR showing no gradient and ECH and GIM showing opposite gradient. The common underestimation over the Indian subcontinent is probably owing to missing aerosol species such as nitrate aerosol (Fig. 6), incorrect meteorological fields such as air temperature and relative humidity, or the underestimation of anthropogenic emissions in these models (discussed in details in Sect. 5).

Starting from the pre-monsoon season (MAM), the entire South Asia is characterized by high AOD mainly due to the mineral dust transported from the arid and desert region by westerly winds, with maximum AOD over the IGP region seen from three satellites (Fig. 7b). It was reported that dust contributes to 62 % of the AOD at Kanpur (Srivastava et al., 2012a). Five models (GE5, GIE, GIM, GOC and SPR) partially capture this spatial distribution. It is interesting that the model HAD shows high AOD over the northern India, which is dominated by nitrate rather than dust (refer to Fig. 6). The dust source in the northwestern parts of South Asia is missing in HAD as shown in Fig. 7b. The model ECH shows very low AOD and little dust over IGP. Despite these deficiencies, model simulations over South Asia during the pre-monsoon season are closer to the satellite data than those during the winter, with the modeled averaged AOD capturing about 71 % of the retrieved ones in the pre-monsoon season compared to only 54 % in the winter.

During the monsoon season (JJAS), the dust transported mainly from the Arabian Peninsula by the strong southwesterly wind explains the high AOD over northwestern India (Fig. 7c). High AOD over the Arabian Sea and southwest Asia is evident from MODIS and MISR. Most models reproduce both the spatial distribution and the amplitude of AOD during this season, indicating that these models have captured dust emission over the Arabian Peninsula and its transport to South Asia. However, it should be noted that during the monsoon season the monthly mean AOD from satellites is

ACPD
14, 19095–19147, 2014

likely to be biased high because only limited number of cloud-free days are available for aerosol retrievals (Ramachandran and Cherian, 2008).

During the post-monsoon season (ON) the southwesterly wind flow significantly becomes weak, thus dust transport to the Indian subcontinent is minimal compared to the pre-monsoon and monsoon seasons. Based on the spatial distributions from the three satellites (Fig. 7d), high AOD is located over the IGP with maxima over western IGP associated with the biomass burning from the agriculture waste fires particularly in this season (Fig. 3). The burning area is mainly located in the northwestern IGP region, such as Punjab, Haryana and western Uttar Pradesh. With the aid of northwesterly winds, aerosols are transported to the central IGP along the valley as well as southward (Badarinath et al., 2009a, b). However, none of the models capture these features, indicating the biomass burning emissions are severely underestimated in the current inventory based on GFED2, which will be discussed in Sect. 5.3. In contrast to the underestimations by other models, HAD overestimated AOD over IGP due to the high amount of nitrate (Fig. 6).

4.4 Aerosol vertical distribution

Figure 8 shows the comparison of modeled vertical aerosol extinction at 550 nm with the CALIOPSO data at 532 nm (namely CALIOP) in 4 seasons. In order to show latitudinal gradient, two representative stations are chosen, with Kanpur in northern India and Hyderabad in central India (refer the locations to Fig. 1). Based on CALIPSO data at Kanpur ($2^\circ \times 2^\circ$ box averaged around the station location) in Fig. 8a, the extinction coefficient reaches the maximum value of 0.4 km^{-1} during the winter at Z_a = 1.05 km, but decreases rapidly upward and diminishes around 4 km. Note that low value near surface in CALIPSO profile may be partly explained by the contamination of the measured signal by the surface return (Koffi et al., 2012). In contrast with the relatively stable lower troposphere in the winter season, boundary layer mixing, convection, and transport are enhanced in pre-monsoon season. As a result, aerosols are more efficiently mixed vertically, with Z_a in CALIPSO increased from 1.05 km in DJF to 2.11 km

ACPD
14, 19095–19147, 2014

in MAM. The aerosol extinction near the surface in MAM is only half of its DJF values, and the fraction of AOD in the lowest 2 km is reduced from 88 % in DJF to 52 % in MAM when the aerosol vertical mixing is relatively uniform within the lowest 3 km and diminishes at higher altitude around 5–6 km. The profile during the monsoon season is similar to that in the pre-monsoon but with a lower value of Z_a as 1.8 km; and the profile during the post-monsoon is similar to that in the winter but with a higher value of Z_a as 1.2 km.

Most models, especially GE5, capture the CALIPSO observed seasonal variation of Z_a (and $F_{2\,km}$) over Kanpur, with lower Z_a (higher $F_{2\,km}$) during the wintertime (DJF) and post-monsoon (ON), and higher Z_a (lower $F_{2\,km}$) during the pre-monsoon (MAM) and monsoon (JJAS) at all stations, although the profiles and amplitudes are quite different from those of CALIPSO. At Kanpur in DJF, most models (except for HAD and GIE) largely underestimate AOD by 57 % (ECH) to 85 % (SPR), in particular the extinction coefficient in the lowest 2 km, with $F_{2\,km}$ varying from 68 % (GIM) to 87 % (GE5) among these 5 models in contrast to 88 % in CALIPSO (Fig. 8a). At Hyderabad in central India during the winter (DJF) and the post-monsoon (ON), models agree with the CALIPSO relatively better. Different from CALIPSO and other models, HAD produces extreme high extinction coefficient close to surface at Kanpur throughout all seasons, about a factor of 2 of CALISPO in DJF and a factor of 10 in ON, so do GIE and GIM in JJAS about a factor of 4 and 7 of CALIPSO, respectively. In addition, there is an abnormal increase of extinction coefficient between 2–3 km in model GIE in all seasons and stations, associated with problems in the nitrate simulation in this model.

4.5 Monthly BC surface concentration

Figure 9 shows observed and modeled monthly surface BC concentration in 2006 (2005 from model ECH) at 8 ICARB stations. In general, the magnitude of BC surface concentrations is closely related to the strength of emission source, with higher values in northern India, gradually decreasing southward. In particular, the highest BC surface concentration is found in the largest Indian city Delhi, with a value of 27 $\mu g\,m^{-3}$

ACPD
14, 19095–19147, 2014

in January. In contrast, BC surface concentration is lower in the remote sites, such as the island sites (Minicoy and Port Blair) and mountain site (Nainital), not exceeding 2.6 $\mu g\,m^{-3}$. In addition, the surface BC concentration exhibits pronounced seasonal variation, with higher values found in the winter and post-monsoon seasons and lower values in the spring and summer. We attribute this temporal variability to the seasonal variations of emission sources, boundary layer depth (affecting vertical mixing), and rainfall (removing BC from the atmosphere). It was reported by previous studies that total BC loading over South Asia in winter mainly comes from biofuel emissions along with coal burning in the vicinity of the measurement location (e.g. Ali et al., 2004; Singh et al., 2008; Beegum et al., 2009; Srivastava et al., 2012b). Overall, modeled BC surface concentrations at all stations except Nainital (a mountain site) are too low especially in winter, varying from near zero to 6 $\mu g\,m^{-3}$. In particular, in Delhi and Hyderabad – two very large cities (see Table 2), all models show a pronounced low bias in the winter, capturing only 3–19 % of the observed values. The simulated BC surface concentrations are found to have a better agreement at Kharagpur, where models capture 20–100 % of the observed value. This contrast is possibly due to the fact that BC loading at Kharagpur mainly comes from coal-fired power plants (Nair et al., 2007), which are relatively well represented in the emission data (discussed in Sect. 5.2). At Minicoy and Port Blair, where the observed BC concentration are relatively lower, models agree better with ICARB, capturing about 10–38 % of the observed values. It should be noted that it is difficult for a global model with a coarse spatial resolution to reproduce pollutant concentrations measured in an urban environment, though it is more reasonable to expect these kinds of models to capture background (e.g. over the mountain site of Nainital and the island sites of Minicoy and Port Blair). Interestingly, despite the low bias of BC concentration, most models reproduce the seasonal variation patterns at these sites with higher concentrations in winter and lower concentrations in summer, similar to what was pointed out in a recent study that compared the ICARB BC data with two models (Moorthy et al., 2013).

ACPD
14, 19095–19147, 2014

5 Possible causes of the aerosol underestimations

As shown above, AOD, AAOD and BC surface concentration are consistently underestimated during the wintertime and the post-monsoon season by the seven global models used in this study. Such underestimation seems to be a quite common problem in other models as well, as shown in other previous studies (e.g. Dickerson et al., 2002; Reddy et al., 2004; Chin et al., 2009; Ganguly et al., 2009; Goto et al., 2011; Cherian et al., 2013). In particular, the AOD and BC surface concentrations are most severely underestimated over the IGP (the main region of anthropogenic emissions). Several possible causes for these underestimates are suggested as below.

5.1 Wintertime relative humidity (RH) over the IGP

Foggy days with high humidity are very common during the wintertime over the IGP region (Gautam et al., 2007). For example, Kanpur was subjected to heavy fog or haze for about > 65 % days in the month of December 2004 (Tripathi et al., 2006), with averaged surface RH averaged about 75 % and the surface temperature about 14.6 °C. Low precipitation thus low wet removal in winter further contributes to accumulation of aerosols (Tripathi et al., 2006).

Figure 10 shows the comparisons between seven models and in-situ measurements from the ISRO-GBP land campaign at four stations in the IGP for December 2004. Comparisons are shown for surface meteorological conditions (RH and temperature); surface aerosol concentrations of SO_4^{2-}, NO_3^-, OA and BC; and column AOD and AAOD. Compared with the measured RH of 75 % at Kanpur, the RH in six of the seven models (all except for HAD) is found significantly low, only 11–35 %. This large underestimation could be partly due to the warm biases of air temperature about 1.7–7.5 °C across models (thus high bias of saturation water vapor pressure and low bias of RH). Under such dry conditions, the hygroscopic growth of soluble aerosols is suppressed. For example, in models GE5 and GOC, mass extinction efficiencies (MEE) of SO_4^{2-} would be almost doubled, and those of OC and NO_3^- would be enhanced by half, if

ACPD
14, 19095–19147, 2014

RH increases from the model averaged 21 % to the observed 75 % (Fig. 11). Note that NO_3^- is to be added to GE5.

In addition, foggy conditions favor the formation of secondary inorganic aerosol through enhanced aqueous-phase reaction, which were supported by the increased aerosol number concentration and surface concentrations of SO_4^{2-} and NO_3^- at Delhi (Tare et al., 2006), Hisar, and Allahabad (Ram et al., 2012), all in the IGP. High RH and lower temperature in the winter also favor the formation of NH_4NO_3 by the reaction of nitric acid (HNO_3) and NH_3 (Lewandowska et al., 2004). The lack of foggy condition in current models would suppress such aqueous phase reactions in the winter, and the exclusion of nitrate aerosols in some of the models would further contribute to the low bias of wintertime AOD.

5.2 Anthropogenic/biofuel emission amounts and seasonal variation

At Kanpur, the observed surface concentration of SO_4^{2-} is 14.9 $\mu g\,m^{-3}$ and NO_3^- is 15.7 $\mu g\,m^{-3}$ as shown in Fig. 10. All models underestimate the surface concentration of SO_4^{2-}, capturing merely 5 % (GIE and GIM) to 50 % (GE5) of the observed SO_4^{2-}. Among the three models that include NO_3^-, GIE and GIM produces extremely low NO_3^- concentrations that is only 0.1 % of the observed amount, whereas HAD captures about 38 % of the observed NO_3^-. Interestingly, among all models, AOD simulated by HAD is the closest to the observations during the winter, which is not only apparent at 4 stations in IGP (Kanpur, Agra, Allahabad and Hisar) (Fig. 10) but also over entire South Asia (Fig. 7a). This is closely associated with its inclusion of NO_3^- (Fig. 6) and aforementioned high relative humidity (Fig. 10). This evidence suggests the contribution of RH and NO_3^- to the high AOD observed over IGP region in the winter. Meanwhile, the model discrepancies also suggests that the simulations of NO_3^- and SO_4^{2-} need to be improved in all models, especially NO_3^- that should be included or improved. At Kanpur, the models also largely underestimate surface OA and BC concentration, capturing only 8 % (GIE and GIM) to 60 %(GE5) of the observed OA values, and 8 %

ACPD
14, 19095–19147, 2014

(GIE and GIM) to 46 % (SPR) of the observed BC values, respectively. The surface concentrations of all species are rather low in the two GISS models (GIE and GIM), usually less than 10 % of observed values. As shown in Fig. 10, the underestimations of surface concentrations by these models are similar at other stations in the IGP, i.e. Agra, Allahabad and Hisar, which differ from Kanpur as being semi-urban and less populated. Therefore, the results above suggest that the anthropogenic emissions used by the models (i.e., A2-ACCMIP and A2-MAP) are likely biased low. For comparison, year 2000 BC emissions over India in A2-ACCMIP and A2-MAP are about 0.5 Tg yr^{-1}, at the low end of a group of emission inventories shown in Granier et al. (2011), with 40 % or 0.3 Tg yr^{-1} lower than those considered by REAS and GAINS-2008 emission inventories (Fig. 5a in Granier et al., 2011). A study by Nair et al. (2012) reported that the simulated BC surface concentration at Kharagpur agreed better with the observations using REAS.

Different from other regions in Northern Hemisphere where fossil fuel burning and industrial processes tend to dominate, biofuel (about 27.0 % energy usage in 2007) and open biomass burning in South Asia contribute two-thirds of carbon-containing aerosols to form the dense brown clouds in the winter (Gustafsson et al., 2009). Over India, 42 % of total BC emission is from biofuel, which is believed to be the largest source of BC, with the rest 33 % from open biomass burning and 25 % from fossil fuel (Venkataraman et al., 2005). This is because the incomplete combustion of residential heating and cooking (burning of wood, paper or other solid wastes) is quite common in South Asia, especially among the underprivileged, leading to large amount of smoke comprised mainly of black carbon and condensed semi-volatile organics. We have found in this study that the simulated BC surface concentrations agree better with the observations at Kharagpur than at Delhi (Fig. 9). As reported by Prasad et al. (2006), the sources of BC at Kharagpur located in eastern IGP were mainly linked to the clusters of the coal-based industries there, while mainly linked to combustion of biofuel at Delhi in western IGP. This contrast is most pronounced in the winter when residential heating is highly demanded, leading to enhanced emissions of biofuel. In sum, the un-

ACPD
14, 19095–19147, 2014

derestimation of anthropogenic emission in South Asia is likely attributed more to the biofuel combustion. As another evidence, the ratios of OC/BC were reported as high as 8.± 2.2 at Allahabad (Ram et al., 2012) and 8.5 ± 2.2 at Hisar (Rengarajan et al., 2007) during December 2004, indicating a major emission source from biomass combustions, such as from biofuel (Husain et al., 2007). However, in the models studied in this paper, the ratios range from only 0.44–4.02 at Allahabad and 0.58–3.80 at Hisar, indicating a domination of source from fossil fuel instead (Husain et al., 2007).

In addition, the anthropogenic emissions of both A2-ACCMIP and A2-MAP emission datasets used by models in this study are constant throughout each year. The lack of seasonal variation would amplify the underestimation of aerosol amount found in models during the winter, when more biofuels are consumed for heating. In fact, the uncertain and inadequate representations of aerosol emissions over South Asia have been pointed out by other studies as well (e.g. Sahu et al., 2008; Ganguly et al., 2009; Nair et al., 2012; Lawrence and Lelieveld, 2010).

5.3 Agriculture waste burning emissions

The extensive agriculture waste burning during post-monsoon season (October–November) after harvest in northwest India (e.g., Punjab) makes a large contribution to the enhanced dense haze over South Asia in this season. The agricultural fire in this area is evident in the MODIS fire count product, which is responsible for the high AOD shown in the satellite products (Vadrevu et al., 2011; Sharma et al., 2010). The smoke from Punjab also impacts the downwind regions by eastward transport along IGP and southward to central-south India (Sharma et al., 2010; Badarinath et al., 2009a, b).

The monthly BC emission from open biomass burning used by most models is 0.011 Tg C yr^{-1} during the post-monsoon season over South Asia, only about 2 % of that from anthropogenic emission (comparing Fig. 3 and Fig. 2). In particular around Lahore, an AERONET station over the northwestern "breadbasket" agriculture region, the open biomass burning emission of BC is only around 0.03 g C m^{-2} yr^{-1}, less than 10 % of that from anthropogenic emission. Such small amount of open biomass burning

ACPD
14, 19095–19147, 2014

emission is indeed questionable because the BC emissions from open biomass burning should be comparable to that from anthropogenic emissions in November, considering a significant enhanced AAOD observed at Lahore in this season (Fig. 5). The underestimation of BC emission from agriculture waste burning implies a similar degree of underestimation of OC from the same source. Therefore, it is not surprising that all models fail to capture high AAOD and AOD in this season (Figs. 5 and 7d).

The open biomass burning emission datasets used in all models during our study period (2000–2007) are based on Global Fire Emissions Database Version 2 (GFED2), which is derived from MODIS burned area products. However, it was previously reported that the small fires such as agricultural waste burning were largely missing in the current GFED product (e.g. van der Werf et al., 2010; Randerson et al., 2012). The area burned in agricultural waste burning area are usually underestimated because the size of agriculture fires is so small that may not generate detectable burned scars in the 500 m pixel resolution of MODIS product (van der Werf et al., 2010; Randerson et al., 2012).

5.4 Other factors

Other factors can also cause the model underestimation of AOD. For example, the observed ratio of water-soluble organic carbon (WSOC) to OC varied from 0.21 to 0.65, suggesting a significant contribution from secondary organic aerosols (SOAs) in India (Ram and Sarin et al., 2010). Enhanced SOA production was actually observed during fog episodes (Kaul et al., 2011). However, only two out of seven models include a detailed SOA chemistry. In addition, although the dust emission is minimal compared with anthropogenic emissions during the wintertime, the mineral sources such as silicates and alumina could be from road traffic dust and soil re-suspension, construction activity in the urban regions of the IGP (Tiwari et al., 2009). However, current models do not include these anthropogenic dust emissions yet.

Some difficulties with the models might be associated with the coarse spatial resolution (i.e. coarser than 1°). Considering the terrain feature over South Asia, especially

ACPD
14, 19095–19147, 2014

the valley-type topography of the IGP region with the towering Himalaya in the north, the aerosol processes may not be adequately represented at such coarse spatial resolution. In addition, because of the non-linearity of wind-dependent dust emission and RH-dependent aerosol hygroscopic growth, a finer model spatial resolution will result in a higher dust emission and AOD (Bian et. al 2009). The observed urban pollution levels at stations, such as Kanpur and Delhi, are expected to be lower in a model box with a coarse spatial resolution (e.g. 1°) than a fine one (e.g. half degree).

Interestingly, the models with the same anthropogenic emissions and biomass burning emissions produce quite different results. At Kanpur in December 2004, for example, surface concentration of OA in the model SPR is 10 times as large as that in GIM (Fig. 10), which uses the same anthropogenic emission data, A2-ACCMIP. Additionally, surface concentration of BC in SPR is 6 times as large as that in GIM (Fig. 10). Two other models, HAD and GOC, use the same A2-MAP emissions, but have noticeably different seasonal variations of sulfate AOD (Fig. 6). Albeit the emission amount usually determines the magnitude of aerosols in the atmosphere, it plays little role in explaining the large model diversities. Instead, the differences in the treatment of atmospheric processes (e.g., wet removal, dry deposition, cloud convection, aqueous-phase oxidation and transport), assumptions of particle size, mixture, water uptake efficiency, and optical properties are more responsible for the inter-model differences.

6 Conclusions

In this study, the aerosol simulations for 2000–2007 from seven global models are evaluated with satellite data and ground-based measurements over South Asia, in particular over Northern India (i.e. IGP), one of the heavily polluted regions in the world. The high AOD over the IGP is associated with high aerosol and precursor gas emissions (such as dust, SO_2, NO_x, NH_3, OA and BC) from local and upwind regions, and its valley-type topography (bounded by the towering Himalaya), favorable for accumu-

ACPD
14, 19095–19147, 2014

lation of both anthropogenic and dust aerosols in this region. The main results of this study are summarized as below.

1. Averaged over the entire South Asia for 2000–2007, the annual mean AOD is about 0.281–0.355 from satellites retrievals. Six out of seven models consistently underestimate the annual mean AOD by 18–45 % compared to MISR, the lowest bound of four satellite datasets. The model performances are worse over northern India where the AOD from the same six models underestimate the annual mean AOD by 20–56 % compared to MISR.

2. In general, the underestimations are mainly found during the winter and post-monsoon months when anthropogenic and open biomass burning emissions are dominant. During wintertime (DJF), six out of seven models largely underestimate AOD over Indian subcontinent. For example, these six models underestimate AOD by a factor of 4 and AAOD by a factor of 2 relative to AERONET at Kanpur, and the largest underestimations of aerosols occur in the lowest 2 km based on the comparisons with aerosol extinction vertical profiles from CALIOP. During the winter and post-monsoon season, BC surface concentrations are severely underestimated at urban cities (such as Delhi) with the models capturing only 3–19 % of the observed values. Performance is better at remotes island sites (such as Minicoy and Port Blair) with the models capturing about 10–38 % the observed values.

3. The surface mass concentrations of all species (SO_4^{2-}, NO_3^-, OA and BC) in the wintertime simulated by models are as small as 0.1–60 % of the observed values, indicating that the mass loading of aerosol is likely underestimated in all these models. In addition to the fact that the AOD and AAOD are also underestimated, it is very likely that anthropogenic emission, especially from biofuel, during the winter is underestimated in the emission dataset (A2-ACCMIP or A2-MAP). The lack of seasonal variation of emissions amplifies the discrepancies in winter.

ACPD
14, 19095–19147, 2014

4. It was also found that the surface concentration of NO_3^- is comparable with SO_4^{2-} at Kanpur and even higher at Agra in observations. However, NO_3^- is either not considered or significantly underestimated by the models, suggesting a need to better represent NO_3^- in the models.

5. The wintertime near-surface relative humidity is found to be significantly low with the model averaged 20 % compared to the observed 70 % in six out of seven models in IGP, which is associated with warm biases found in air temperature. As a result, the hygroscopic growth of soluble aerosols and formation of secondary inorganic aerosol (NO_3^- and SO_4^{2-}) can be underestimated, which may further lead to an underestimation of AOD in these models.

6. During the post-monsoon season (ON), none of the models capture the observed high AOD over western and central IGP. Such discrepancy is attributed largely to the underestimation of open biomass burning in the emission inventory, which misses the aerosol emissions from agricultural waste burning.

In summary, it remains a challenge for global models to represent the aerosol distributions, loadings and seasonal cycles in South Asia, due to our limited knowledge of the aerosol sources and physical and optical properties, as well as unconstrained model parameters to adequately represent the atmospheric processes. This study identifies the major discrepancies associated with aerosol simulation in state-of-the-art global climate models, and suggests some directions to improve model simulation over South Asia by improving temperature and relative humidity in the meteorological fields, revising biofuel and agriculture fire emission dataset, and including/improving NO_3^- (and SOA). Moreover, more systematic measurements, especially long-term surface and vertical characterization of aerosol composition, precursor gases, optical properties, and meteorological fields (such as temperature, winds, relative humidity), are needed.

ACPD
14, 19095–19147, 2014

Acknowledgements. We thank the ICARB, ISRO-GBP, and AERONET networks for making their data available. Site PIs and data managers of those networks are gratefully acknowledged. We also thank the Goddard Earth Science Data and Information Services Center for providing gridded satellite products of SeaWiFS, MISR, and MODIS through their Giovanni website, and the AeroCom data management for providing access to the global model output used in this study. Brigitte Koffi is appreciated for providing L3 CALIOP data. X. Pan is supported by an appointment to the NASA Postdoctoral Program at the GSFC, administered by Oak Ridge Associated Universities through a contract with NASA. The work by MC, HB, DK, and PC are supported by the NASA MAP and ACMAP Programs. SEB and KT have been supported by the NASA MAP program (NN-H-04-Z-YS-008-N and NN-H-08-Z-DA-001-N). L. Pozzoli was supported by PEGASOS (FP7-ENV-2010-265148). Resources supporting this work were provided by the NASA High-End Computing (HEC) Program through the NASA Center for Climate Simulation (NCCS) at Goddard Space Flight Center. ECHAM5-HAMMOZ simulations were supported by the Deutsches Klimarechenzentrum (DKRZ) and the Forschungszentrum Juelich.

References

Ali, K., Momin, G. A., Tiwari, S., Safai, P. D., Chate, D. M., and Rao, P. S. P.: Fog and precipitation chemistry at Delhi, North India, Atmos. Environ., 38, 4215–4222, 2004.

Badarinath, K. V. S., Kharol, S. K., and Sharma, A. R.: Long-range transport of aerosols from agriculture crop residue burning in Indo-Gangetic Plains – A study using LIDAR, ground measurements and satellite data, J. Atmos. Sol. Terr. Phys., 71, 112–120, doi:10.1016/j.jastp.2008.09.035, 2009a.

Badarinath, K. V. S., Kharol, S. K., Sharma, A. R., and Krishna Prasad, V.: Analysis of aerosol and carbon monoxide characteristics over Arabian Sea during crop residue burning period in the Indo-Gangetic Plains using multi-satellite remote sensing datasets, J. Atmos. Solar-Terr. Phys., 71, 1267–1276, 2009b.

Babu, S. S., Manoj, M. R., Moorthy, K. K., Gogoi, M. M., Nair, V. S., Kumar Kompalli, S., Satheesh, S. K., Niranjan, K., Ramagopal, K., Bhuyan, P. K., and Singh, D.: Trends in aerosol optical depth over indian region: potential causes and impact indicators, J. Geophys. Res. Atmos., 118, 11794–11806, doi:10.1002/2013JD020507, 2013.

ACPD
14, 19095–19147, 2014

Bauer, S. E., Wright, D. L., Koch, D., Lewis, E. R., McGraw, R., Chang, L.-S., Schwartz, S. E., and Ruedy, R.: MATRIX (Multiconfiguration Aerosol TRacker of mIXing state): an aerosol microphysical module for global atmospheric models, Atmos. Chem. Phys., 8, 6003-6035, doi:10.5194/acp-8-6003-2008, 2008.

Bauer, S. E., Menon, S., Koch, D., Bond, T. C., and Tsigaridis, K.: A global modeling study on carbonaceous aerosol microphysical characteristics and radiative effects, Atmos. Chem. Phys., 10, 7439–7456, doi:10.5194/acp-10-7439-2010, 2010.

Beegum, S., Moorthy, S. N., Babu, K. K.,Satheesh, S. S., Vinoj, S. K., Badarinath, V., Safai, K. V. S., Devara, P. D., Singh, P. C. S., Vinod, S., Dumka U. C., and Pant, P.: Spatial distribution of aerosol black carbon over India during pre-monsoon season, Atmos. Environ., 43, 1071–1078, 2009.

Bellouin, N., Rae, J., Jones, A., Johnson, C., Haywood, J., and Boucher, O.: Aerosol forcing in the Climate Model Intercomparison Project (CMIP5) simulations by HadGEM2-ES and the role of ammonium nitrate, J. Geophys. Res., 116, D20206, doi:10.1029/2011JD016074, 2011.

Bian, H., Chin, M., Rodriguez, J. M., Yu, H., Penner, J. E., and Strahan, S.: Sensitivity of aerosol optical thickness and aerosol direct radiative effect to relative humidity, Atmos. Chem. Phys., 9, 2375–2386, doi:10.5194/acp-9-2375-2009, 2009.

Cherian, R., Venkataraman, C., Quaas, J., and Ramachandran, S.: GCM simulations of anthropogenic aerosol-induced changes in aerosol extinction, atmospheric heating and precipitation over India, J. Geophys. Res. Atmos., 118, 2938–2955, doi:10.1002/jgrd.50298, 2013.

Chin, M., Ginoux, P., Kinne, S., Torres, O., Holben, B. N., Duncan, B. N., Martin, R. V., Logan, J. A., Higurashi, A., and Nakajima, T.: Tropospheric aerosol optical thickness from the GOCART model and comparisons with satellite and sun photometer measurements, J. Atmos. Sci., 59, 461–483, 2002.

Chin, M., Diehl, T., Dubovik, O., Eck, T. F., Holben, B. N., Sinyuk, A., and Streets, D. G.: Light absorption by pollution, dust and biomass burning aerosols: A global model study and evaluation with AERONET data, Ann. Geophys., 27, 3439–3464, 2009, http://www.ann-geophys.net/27/3439/2009/.

Chin, M., Diehl, T., Tan, Q., Prospero, J. M., Kahn, R. A., Remer, L. A., Yu, H., Sayer, A. M., Bian, H., Geogdzhayev, I. V., Holben, B. N., Howell, S. G., Huebert, B. J., Hsu, N. C., Kim, D., Kucsera, T. L., Levy, R. C., Mishchenko, M. I., Pan, X., Quinn, P. K., Schuster, G. L., Streets, D. G., Strode, S. A., Torres, O., and Zhao, X.-P.: Multi-decadal aerosol variations from

ACPD
14, 19095–19147, 2014

1980 to 2009: a perspective from observations and a global model, Atmos. Chem. Phys., 14, 3657–3690, doi:10.5194/acp-14-3657-2014, 2014.
Colarco, P., da Silva, A., Chin, M., and Dieh, T. I.: Online simulations of global aerosol distributions in the NASA GEOS-4 model and comparisons to satellite and ground-based aerosol optical depth, J. Geophys. Res., 115, D14207, doi:10.1029/2009JD012820, 2010.
Das, S. K., Jayaraman, A., and Misra, A.: Fog-induced variations in aerosol optical and physical properties over the Indo-Gangetic Basin and impact to aerosol radiative forcing, Ann. Geophys., 26, 1345–1354, doi:10.5194/angeo-26-1345-2008, 2008.
Dickerson, R. R., Andreae, M. O., Campos, T., Mayol-Bracero, O. L., Neususess, C., and Streets, D. G.: Analysis of black carbon and carbonmonoxide observed over the Indian Ocean: Implications for emissions and photochemistry, J. Geophys. Res., 107, 8017, doi:10.1029/2001JD000501, 2002.
Diehl, T., Heil, A., Chin, M., Pan, X., Streets, D., Schultz, M., and Kinne, S.: Anthropogenic, biomass burning, and volcanic emissions of black carbon, organic carbon, and SO_2 from 1980 to 2010 for hindcast model experiments, Atmos. Chem. Phys. Discuss., 12, 24895–24954, doi:10.5194/acpd-12-24895-2012, 2012.
Ganguly, D., Jayaraman, A., Rajesh, T. A., and Gadhavi, H.: Wintertime aerosol properties during foggy and nonfoggy days over urban center Delhi and their implications for shortwave radiative forcing, J. Geophys. Res., 111, D15217, doi:10.1029/2005JD007029, 2006.
Ganguly, D., Ginoux, P., Ramaswamy, V., Winker, D. M., Holben, B. N., and Tripathi, S. N.: Retrieving the composition and concentration of aerosols over the Indo-Gangetic basin using CALIOP and AERONET data, Geophys. Res. Lett., 36, L13806, doi:10.1029/2009GL038315, 2009.
Gautam, R., Hsu, N. C., Kafatos, M., and Tsay, S.-C.: Influences of winter haze on fog/low cloud over the Indo-Gangetic Plains, J. Geophys. Res., 112, D05207, doi:10.1029/2005JD007036, 2007.
Gautam, R., Hsu, N. C., Lau, W. K.- M., and Yasunari, T. J.: Satellite observations of desert dust-induced Himalayan snow darkening, Geophys. Res. Lett., 40, 988–993, doi:10.1002/grl.50226, 2013.
Girolamo, D. L., Bond, T. C., Bramer, D., Diner, D. J., Fettinger, F., Kahn, R. A., Martonchik, J. V., Ramana, M. V., Ramanathan, V., and Rasch, P. J.: Analysis of Multi-angle Imaging SpectroRadiometer (MISR) aerosol optical depths over greater India during winter 2001–2004, Geophys. Res. Lett., 31, L23115, doi:10.1029/2004GL021273, 2004.

ACPD
14, 19095–19147, 2014

Goto, D., Takemura, T., Nakajima, T., and Badarinath, K. V. S.: Global aerosol model-derived black carbon concentration and single scattering albedo over Indian region and its comparison with ground observations, Atmos. Environ., 45, 3277–3285, 2011.

Granier, C., Bessagnet, B., Bond, T., D'Angiola, A., van der Gon, H. D., Frost, G. J., Heil, A., Kaiser, J. W., Kinne, S., Klimont, Z., Kloster, S., Lamarque, J.-F., Liousse, C., Masui, T., Meleux, F., Mieville, A., Ohara, T., Raut, J. C., Riahi, K., Schultz, M. G., Smith, S. J., Thompson, A., van Aardenne, J., van der Werf, G. R., and van Vuuren, D. P.: Evolution of anthropogenic and biomass burning emissions of air pollutants at global and regional scales during the 1980–2010 period, Climatic Change, 109, 163–190, doi:10.1007/s10584-011-0154-1, 2011.

Gustafsson, Ö., Kruså, M., Zencak, Z., Sheesley, R. J., Granat, L., Engström, E., Praveen, P. S., Rao, P. S. P., Leck, C., and Rodhe, H.: Brown clouds over South Asia: Biomass or fossil fuel combustion?, Science, 323, 495–498, 2009.

Holben, B. N., Eck, T. F., Slutsker, I., Tanre, D., Buis, J. P., Setzer, A., Vermote, E., Reagan, J. A., Kaufman, Y. J., Nakajima, T., Lavenu, F., Jankowiak, I., and Smirnov, A.: AERONET – a federated instrument network and data archive for aerosol characterization, Remote Sens. Environ., 66, 1–16, 1998.

Hsu, N. C., Tsay, S.-C., King, M. D., and Herman, J. R.: Deep Blue retrievals of Asian aerosol properties during ACE-Asia, IEEE T. Geosci. Remote Sens., 44, 3180–3195, 2006.

Hsu, N. C., Gautam, R., Sayer, A. M., Bettenhausen, C., Li, C., Jeong, M. J., Tsay, S.-C., and Holben, B. N.: Global and regional trends of aerosol optical depth over land and ocean using SeaWiFS measurements from 1997 to 2010, Atmos. Chem. Phys., 12, 8037–8053, doi:10.5194/acp-12-8037-2012, 2012.

Husain, L., Dutkiewicz, V. A., Khan, A. J., Chin, M., and Ghauri, B. M.: Characterization of carbonaceous aerosols in urban air, Atmos. Envrion., 41, 6872–6883, 2007.

Jethva, H., Satheesh, S. K., Srinivasan, J., and Krishnamoorthy, K.: How good is the assumption about visible surface reflectance in MODIS aerosol retrieval over land? A comparison with aircraft measurements over an urban site in India, IEEE T. Geosci. Remote., 47, 1990–1998, 2009.

Kahn, R. A.,Li, W.-H.,Moroney, C., Diner, D. J., Martonchik, J. V., and Fishbein, E.: Aerosol source plume physical characteristics from space-based multiangle imaging, J. Geophys. Res., 112, D11205, doi:10.1029/2006JD007647, 2007.

ACPD
14, 19095–19147, 2014

Kaskaoutis, D. G., Singh, R. P., Gautam, R., Sharma, M., Kosmopoulos, P. G., Tripathi, S. N.: Variability and trends of aerosol properties over Kanpur, northern India using AERONET data (2001–10), Environ. Res. Lett., 109, 024003, doi:10.1088/1748-9326/7/2/024003, 2012.
Kaul, D., Gupta T., Tripathi, S. N., Tare, V., and Collett, J.: Secondary Organic Aerosol: A comparison between foggy and non-foggy days, Environ. Sci. Technol., 45, 7307–7313, 2011.
Kaul, D. S., Gupta, T., Tripathi, S. N., Tare, V., and Collett, J. L.: Secondary organic aerosol: a comparison between foggy and nonfoggy days, Environ Sci Technol., 45, 7307-13, doi:10.1021/es201081d, 2011.
Koffi, B., Schulz, M., Bréon, F.-M., Griesfeller, J., Winker, D., Balkanski, Y., Bauer, S., Berntsen, T., Chin, M., Collins, W. D., Dentener, F., Diehl, T., Easter, R., Ghan, S., Ginoux, P., Gong, S., Horowitz, L. W., Iversen, T., Kirkevåg, A., Koch, D., Krol, M., Myhre, G., Stier, P., and Takemura, T.: Application of the CALIOP layer product to evaluate the vertical distribution of aerosols estimated by global models: AeroCom phase I results, J. Geophys. Res., 117, D10201, doi:10.1029/2011JD016858, 2012.
Lau, K. M., Kim, M. K., and Kim, K. M.: Asian summer monsoon anomalies induced by aerosol direct forcing: The role of the Tibetan Plateau, Clim. Dyn., 26, 855-864, 2006.
Lau, K. M., Kim, M. K., Kim, K. M., and Lee, W. S.: Enhanced surface warming and accelerated snow melt in the Himalayas and Tibetan Plateau induced by absorbing aerosols, Env. Res. Lett., 5, 025204, doi:10.1088/1748-9326/5/2/025204, 2010.
Lawrence, M. G. and Lelieveld, J.: Atmospheric pollutant outflow from southern Asia: a review, Atmos. Chem. Phys., 10, 11017–11096, doi:10.5194/acp-10-11017-2010, 2010.
Lewandowska, A., Lucyna, F., and Magdalena, B.: Ammonia and ammonium over the southern Baltic Sea, part 2. The origin of ammonia and ammonium over two stations: Gdynia and Hel, Oceanologia, 46, 185–200, 2004.
Levy, R. C., Remer, L. A., Kleidman, R. G., Mattoo, S., Ichoku, C., Kahn, R., and Eck, T. F.: Global evaluation of the Collection 5 MODIS dark-target aerosol products over land, Atmos. Chem. Phys., 10, 10399–10420, doi:10.5194/acp-10-10399-2010, 2010.
Martonchik, J. V., Diner, D. J., Kahn, R., Gaitley, B., and Holben, B. N.: Comparison of MISR and AERONET aerosol optical depths over desert sites, Geophys. Res. Lett., 31, L16102, doi:10.1029/2004GL019807, 2004.
Menon, S., Koch, D., Beig, G., Sahu, S., Fasullo, J., and Orlikowski, D.: Black carbon aerosols and the third polar ice cap, Atmos. Chem. Phys., 10, 4559–4571, doi:10.5194/acp-10-4559-2010, 2010.

ACPD
14, 19095–19147, 2014

Moorthy, K. K., Beegum, S. N., Srivastava, N., Satheesh, S. K., Chin, M., Blond, N., Babu, S. S., and Singh, S.: Performance evaluation of chemistry transport models over India, Atmos. Environ., 71, 210–225, 2013.

Myhre, G., Samset, B. H., Schulz, M., Balkanski, Y., Bauer, S., Berntsen, T. K., Bian, H., Bellouin, N., Chin, M., Diehl, T., Easter, R. C., Feichter, J., Ghan, S. J., Hauglustaine, D., Iversen, T., Kinne, S., Kirkevåg, A., Lamarque, J.-F., Lin, G., Liu, X., Lund, M. T., Luo, G., Ma, X., van Noije, T., Penner, J. E., Rasch, P. J., Ruiz, A., Seland, Ø., Skeie, R. B., Stier, P., Takemura, T., Tsigaridis, K., Wang, P., Wang, Z., Xu, L., Yu, H., Yu, F., Yoon, J.-H., Zhang, K., Zhang, H., and Zhou, C.: Radiative forcing of the direct aerosol effect from AeroCom Phase II simulations, Atmos. Chem. Phys., 13, 1853–1877, doi:10.5194/acp-13-1853-2013, 2013.

Nair, V. S., Moorthy, K. K., Alappattu, D. P., Kunhikrishnan, P. K., George, S., Nair, P. R., Babu, S. S., Abish, B., Satheesh, S. K., Tripathi, S. N., Niranjan, K., Madhavan, B. L., Srikant, V., Dutt, C. B. S., Badarinath, K. V. S., and Reddy, R. R.: Wintertime aerosol characteristics over the Indo-Gangetic Plain (IGP): impacts of local boundary layer processes and long-range transport, J. Geophys. Res., 112, D13205, doi:10.1029/2006JD008099, 2007.

Nair, V. S., Solmon, F., Giorgi, F., Mariotti, L., Babu, S. S., and Moorthy, K. K.: Simulation of South Asian aerosols for regional climate studies, J. Geophys. Res., 117, D04209, doi:10.1029/2011JD016711, 2012.

Ohara, T., Akimoto, H., Kurokawa, J., Horii, N.,Yamaji, K., Yan, X., and Hayasaka, T. : An Asian emission inventory of anthropogenic emission sources for the period 1980–2020, Atmos. Chem. Phys., 7, 4419–4444, 2007, http://www.atmos-chem-phys.net/7/4419/2007/.

Pozzoli, L., Janssens-Maenhout, G., Diehl, T., Bey, I., Schultz, M. G., Feichter, J., Vignati, E., and Dentener, F.: Reanalysis of tropospheric sulphate aerosol and ozone for the period 1980–2005 using the aerosol-chemistry-climate model ECHAM5-HAMMOZ, Atmos. Chem. Phys. Discuss., 11, 10191–10263, doi:10.5194/acpd-11-10191-2011, 2011.

Prasad, A. K., Singh, R. P., and Kafatos, M.: Influence of coal based thermal power plants on aerosol optical properties in the Indo-Gangetic basin, Geophys. Res. Lett., 33, L05805, doi:10.1029/2005GL023801, 2006.

Qian, Y., Flanner, M. G., Leung, L. R., and Wang, W.: Sensitivity studies on the impacts of Tibetan Plateau snowpack pollution on the Asian hydrological cycle and monsoon climate, Atmos. Chem. Phys., 11, 1929–1948, doi:10.5194/acp-11-1929-2011, 2011.

ACPD
14, 19095–19147, 2014

Ram K. and Sarin, M. M.: Spatio-temporal variability in atmospheric abundances of EC, OC and WSOC over Northern India, J. Aerosol Sci., 41, 88–98, 2010.
Ram, K., Sarin, M. M., Sudheer, A. K., and Rengarajan, R.: Carbonaceous and secondary inorganic aerosols during wintertime fog and haze over urban sites in the Indo-Gangetic Plain, Aerosol Air Qual. Res., 12, 359–370, 2012.
Ramachandran, S., Rengarajan, R., Jayaraman, A., Sarin, M. M., and Das, S. K.: Aerosol radiative forcing during clear, hazy, and foggy conditions over a continental polluted location in north India, J. Geophys. Res., 111, D20214, doi:10.1029/2006JD007142, 2006.
Ramachandran, S. and Cherian R.: Regional and seasonal variations in aerosol optical characteristics and their frequency distributions over India during 2001–2005, J. Geophys. Res., 113, D08207, doi:10.1029/2007JD008560, 2008.
Ramachandran, S. and Kedia S.: Aerosol, clouds and rainfall: inter-annual and regional variations over India, Clim. Dyn., 40(7–8), 1591–1610, doi:10.1007/s00382-012-1594-7, 2013.
Ramanathan, V., Crutzen, P. J., Lelieveld, J., Mitra, A. P., Althausen, D., Anderson, J., Andreae, M. O., Cantrell, W., Cass, G. R., Chung, C. E., Clarke, A. D., Coakley, J. A., Collins, W. D., Conant, W. C., Dulac, F., Heintzenberg, J., Heymsfield, A. J., Holben, B., Howell, S., Hudson, J., Jayaraman, A., Kiehl, J. T., Krishnamurti, T. N., Lubin, D., McFarquhar, G., Novakov, T., Ogren, J. A., Podgorny, I. A., Prather, K., Priestley, K., Prospero, J. M., Quinn, P. K., Rajeev, K., Rasch, P., Rupert, S., Sadourny, R., Satheesh, S. K., Shaw, G. E., Sheridan, P., and Valero, F. P. J.: Indian Ocean Experiment: an integrated analysis of the climate forcing and effects of the great Indio-Asian haze, J. Geophys. Res., 106, 28371–28398, 2001.
Ramanathan, V., Chung, C., Kim, D., Bettge, T., Buja, L., Kiehl, J. T., Washington, W. M., Fu, Q., Sikka, D. R., and Wild, M.: Atmospheric brown clouds: impact on South Asian climate and hydrologic cycle, Proc. Natl. Acad. Sci., 102:5326–5333, doi:10.1073/pnas.0500656102, 2005.
Randerson, J. T., Chen, Y., van der Werf, G. R., Rogers, B. M., and Morton, D. C.: Global burned area and biomass burning emissions from small fires, J. Geophys. Res., 117, G04012, doi:10.1029/2012JG002128, 2012.
Reddy, M. S., Boucher, O., Venkataraman, C., Verma, S., Le'on, J.-F., Bellouin, N., and Pham, M.: General circulation model estimates of aerosol transport and radiative forcing during the Indian Ocean Experiment, J. Geophys. Res., 109, D16205, doi:10.1029/2004JD004557, 2004.

ACPD
14, 19095–19147, 2014

Rengarajan, R., Sarin, M. M., and Sudheer, A. K.: Carbonaceous and inorganic species in atmospheric aerosols during wintertime over urban and high-altitude sites in North India, J. Geophys. Res., 112, D21307, doi:10.1029/2006JD008150, 2007.

Safai, P. D., Kewat, S., Pandithurai, G., Praveen, P. S., Ali, K., Tiwari, S., Rao, P. S. P., Budhawant, K. B., Saha, S. K., and Devara, P. C. S.: Aerosol characteristics during winter fog at Agra, North India, J. Atmos. Chem., 61, 101–118, 2008.

Sahu, S. K., Beig. G., and Sharma, C.: Decadal growth of black carbon emissions in India, Geophys. Res. Lett., 35, L02807, doi:10.1029/2007GL032333, 2008.

Sanap, S. D., Ayantika, D. C., Pandithurai, G., and Niranjan, K.: Assessment of the aerosol distribution over Indian subcontinent in CMIP5 models, Atmospheric Environment, 87, 123–137, 2014.

Sayer, A. M., Hsu, N. C., Bettenhausen, C., Ahmad, Z., Holben, B. N., Smirnov, A., Thomas, G. E., and Zhang, J.: SeaWiFS Ocean Aerosol Retrieval (SOAR): algorithm, validation, and comparison with other datasets, J. Geophs. Res, 117, D03206, doi:10.1029/2011JD016599, 2012.

Sharma, A. R., Kharol, S. K., Badarinath, K. V. S., and Singh, D.: Impact of agriculture crop residue burning on atmospheric aerosol loading – a study over Punjab State, India, Ann. Geophys., 28, 367–379, 2010, http://www.ann-geophys.net/28/367/2010/.

Singh, T., Khillare, P. S., Shridhar, V., and Agarwal, T.: Visibility impairing aerosols in the urban atmosphere of Delhi, Environ. Monit. Assess., 141, 67–77, 2008.

Srivastava, A. K., Tripathi, S. N., Dey, S., Kanawade, V. P., and Tiwari, S.: Inferring aerosol types over the Indo-Gangetic Basin from ground based sunphotometer measurements, Atmos. Res., 109–110, 64–75, doi:10.1016/j.atmosres.2012.02.010, 2012a.

Srivastava, A. K., Singh, S., Pant, P., and Dumka, U. C.: Characteristics of black carbon over Delhi and Manora Peak – a comparative study, Atmos. Sci. Lett., 13, 223–230, doi:10.1002/asl.386, 2012b.

Takemura, T., Nozawa, T., Emori, S., Nakajima, T. Y., and Nakajima,T.: Simulation of climate response to aerosol direct and indirect effects with aerosol transport-radiation model, J. Geophys.Res.-Atmos., 110, D02202, doi:10.1029/2004jd005029, 2005.

Takemura, T., Egashira, M., Matsuzawa, K., Ichijo, H., O'ishi, R., and Abe-Ouchi, A.: A simulation of the global distribution and radiative forcing of soil dust aerosols at the Last Glacial Maximum, Atmos. Chem. Phys., 9, 3061–3073, doi:10.5194/acp-9-3061-2009, 2009.

ACPD
14, 19095–19147, 2014

Tare, V., Tripathi, S. N., Chinnam, N., Srivastava, A. K., Dey, S., Manar, M., Kanawade, V. P., Agarwal, A., Kishore, S., Lal, R. B., Sharma, M.: Measurements of atmospheric parameters during Indian Space Research Organization Geosphere Biosphere Program Land Campaign II at a typical location in the Ganga Basin: 2. Chemical properties, J. Geophys. Res., 111, D23210, doi:10.1029/2006JD007279, 2006.

Tiwari, S., Srivastava, A. K., Bisht, D. S., Bano, T., Singh, S., Behura, S., Srivastava, M. K., Chate, D. M., and Padmanabhamurty, B.: Black carbon and chemical characteristics of PM_{10} and $PM_{2.5}$ at an urban site of North India, J. Atmos. Chem., 62, 193–209, doi:10.1007/s10874-010-9148-z, 2009.

Tripathi, S. N., Dey, S., Tare, V., and Satheesh, S. K.: Aerosol black carbon radiative forcing at an industrial city in northern India, Geophys. Res. Lett., 32, L08802, doi:10.1029/2005GL022515, 2005.

Tripathi, S. N., Tare, V., Chinnam, N., Srivastava, A. K., Dey, S., Agarwal, A., Kishore, S., Lal, R. B., Manar, M., Kanwade, V. P., Chauhan, S. S. S., Sharma, M., Reddy, R. R., Gopal, K. R., Narasimhulu, K., Reddy, L. S. S., Gupta, S., and Lal, S.: Measurements of atmospheric parameters during Indian Space Research Organization Geosphere Biosphere Programme Land Campaign II at a typical location in the Ganga basin: 1. Physical and optical properties, J. Geophys. Res., 111, D23209, doi:10.1029/2006JD007278, 2006.

Tsigaridis, K., Koch, D. M., and Menon, S.: Uncertainties and importance of sea-spray composition on aerosol direct and indirect effects, J. Geophys. Res., 118, 220–235, doi:10.1029/2012JD018165, 2013.

Vadrevu, K. P., Ellicott, E., Badarinath, K. V. S., and Vermote, E.: MODIS derived fire characteristics and aerosol optical depth variations during the agricultural residue burning season, north India, Environ. Pollut., 159, 1560–1569, 2011.

Vadrevu, K. P., Giglio, L., and Justice, C.: Satellite based analysis of fire–carbon monoxide relationships from forest and agricultural residue burning (2003–2011), Atmos. Environ., 64, 179–191, 2013.

van der Werf, G. R., Randerson, J. T., Giglio, L., Collatz, G. J., Mu, M., Kasibhatla, P. S., Morton, D. C., DeFries, R. S., Jin, Y., and van Leeuwen, T. T.: Global fire emissions and the contribution of deforestation, savanna, forest, agricultural, and peat fires (1997–2009), Atmos. Chem. Phys., 10, 11707–11735, doi:10.5194/acp-10-11707-2010, 2010.

ACPD
14, 19095–19147, 2014

Venkataraman, C., Habib, G., Eiguren-Fernandez, A., Miguel, A. H., and Friedlander, S. K.: Residential biofuels in South Asia: carbonaceous aerosol emissions and climate impacts, Science, 307, 1454–1456, 2005

Venkataraman, C., Habib, G., Kadamba, D., Shrivastava, M., Leon, J.-F., Crouzille, B., Boucher, O., and Streets, D. G.: Emissions from open biomass burning in India: Integrating the inventory approach with high-resolution Moderate Resolution Imaging Spectroradiometer (MODIS) active-fire and land cover data, Global Biogeochem. Cycles, 20, GB2013, doi:10.1029/2005GB002547, 2006.

Yasunari, T. J., Bonasoni, P., Laj, P., Fujita, K., Vuillermoz, E., Marinoni, A., Cristofanelli, P., Duchi, R., Tartari, G., and Lau, K.-M.: Estimated impact of black carbon deposition during pre-monsoon season from Nepal Climate Observatory – Pyramid data and snow albedo changes over Himalayan glaciers, Atmos. Chem. Phys., 10, 6603–6615, doi:10.5194/acp-10-6603-2010, 2010.

ACPD

14, 19095–19147, 2014

Table 1. General information of multi-models.

Model	ID	Time range	Res. [a]	Anthrop. Emi. [b]	BB Emi. [c]	Met. Field	Extra[d] Species	References
HadGEM2	HAD	2000–2006	1.8 × 1.2 × 38	A2-MAP	GFED2	ERA-Interim	NO_3^-, SOA	Bellouin et al. (2011)
GOCART-v4	GOC	2000–2007	2.5 × 2 × 30	A2-MAP	GFED2	GEOS-DAS	–	Chin et al. (2002, 2009)
ECHAM5-HAMMOZ	ECH	2000–2005	1.8 × 1.8 × 31	A2-MAP	GFED2	ECMWF analysis	SOA	Pozzoli et al. (2011)
GISS-modelE	GIE	2000–2008	2.5 × 2 × 40	A2-ACCMIP	GFED2	NCEP wind,	NO_3^-, SOA	Tsigaridis et al. (2013)
GISS-MATRIX	GIM	2000–2007	2.5 × 2 × 40	A2-ACCMIP	GFED2	NCEP-wind	NO_3^-	Bauer et al. (2008, 2010)
SPRINTARS	SPR	2000–2008	1.1 × 1.1 × 56	A2-ACCMIP	GFED2	NCEP/NCAR	–	Takemura et al. (2005, 2009)
GEOS5-GOCART	GE5	2000–2008	2.5 × 2 × 72	A2-ACCMIP	GFED2	MERRA	–	Colarco et al. (2010)

[a] Spatial resolutions (° latitude x ° longitude x number of vertical levels).
[b] Anthropogenic emission data are from either A2-ACCMIP or A2-MAP refer to Diehl et al. (2012).
[c] Biomass burning emission data refer to Diehl et al. (2012).
[d] Extra aerosols, either SOA (secondary organic aerosol) or NO_3^-(nitrate), besides commonly included aerosol species, i.e. SO_4^{2-} (sulfate), Dust, SS (sea salt), BC (black carbon), and OA(organic aerosol).

ACPD
14, 19095–19147, 2014

Table 2. Summary of stations in South Asia used in this study.

Type	Station [a]	Lat	Lon	Alt (m)	Population [b] (milli-)	Data Source [c]	Data Category	Main Feature
Urban	Delhi	28.58° N	77.20° E	260	16.75	ICARB	BC	In western IGP, the largest city in India
	Karachi	24.87° N	67.03° E	49	13	AERONET	AOD AAOD	Coastal location in southern Pakistan
	Lahore	31.54° N	74.32° E	270	9	AERONET	AOD AAOD	In western IGP, major agricultural region
	Hyderabad	17.48° N	78.40° E	545	6.81	ICARB	BC	In central Indian Peninsula
	Pune	18.52° N	73.85° E	559	5.05	ICARB	BC	In western plateau
	Kanpur	26.51° N	80.23° E	123	2.77	AERONET/ ISRO-GBP	Misc.[d]	In central IGP
	Agra	27.06° N	78.03° E	169	1.75	ISRO-GBP	Misc.[d]	Between Delhi and Kanpur
	Allahabad	25.45° N	81.85° E	98	1.22	ISRO-GBP	Misc.[d]	In central-eastern IGP
Semi-Urban	Kharagpur	22.52° N	87.52° E	28	0.37	ICARB	BC	In eastern IGP-outflow region to Bay of Bengal
	Hisar	29.09° N	75.42° E	41	0.3	ISRO-GBP	Misc.[d]	Surrounded by agricultural field in western IGP
	Trivandrum	8.55° N	76.90° E	3	0.75	ICARB	BC	A coastal station in southern India
Remote	Port Blair	11.63° N	92.70° E	60	0.1	ICARB	BC	Island in Bay of Bengal
	Nainital	29.20° N	79.30° E	1950	0.04	ICARB	BC	High altitude remote location in the Himalayan foothills
	Minicoy	8.30° N	70.00° E	1	0.009	ICARB	BC	Island in Arabian Sea

[a] In an order of the population.
[b] Statistics in 2011 from wikipedia.
[c] Details in Sect. 3.2 and 3.3.
[d] Miscellaneous, including meteorological fields, AOD, AAOD and aerosol surface concentration.

ACPD
14, 19095–19147, 2014

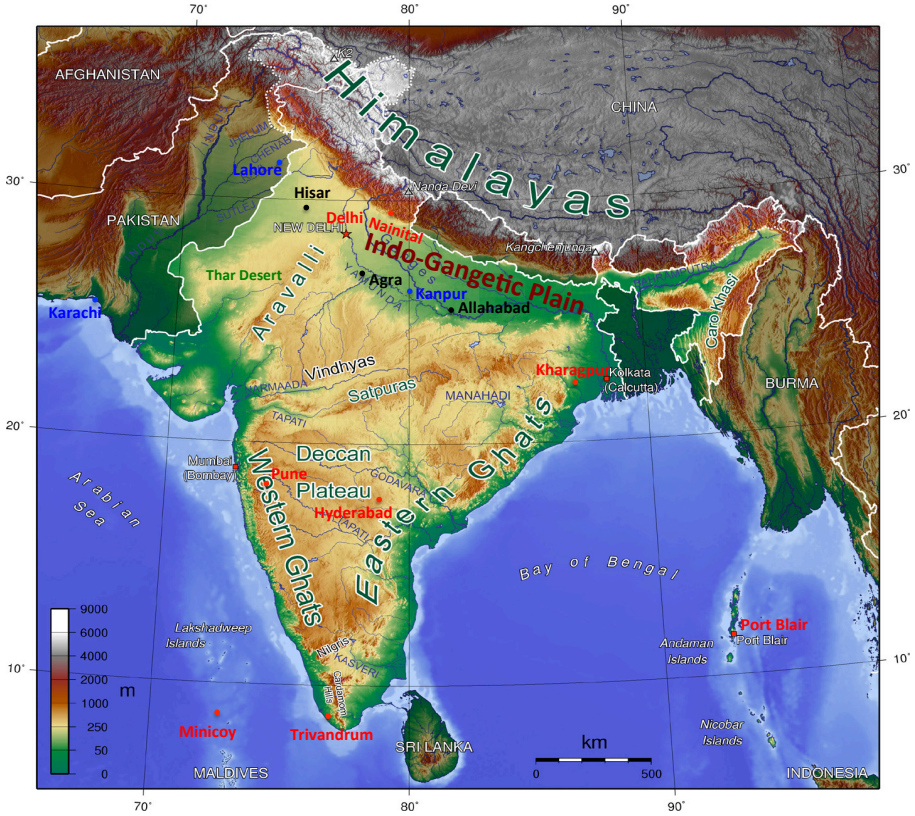

Figure 1. Topography of South Asia overlapped with stations used in this study. Three AERONET stations are labeled in blue, eight ICARB stations in red and four ISRO-GBP stations in black except Kanpur. Topography map is obtained from http://mapofasia.blogspot.com/2013/02/map-of-south-asia-area-pictures.html.

ACPD
14, 19095–19147, 2014

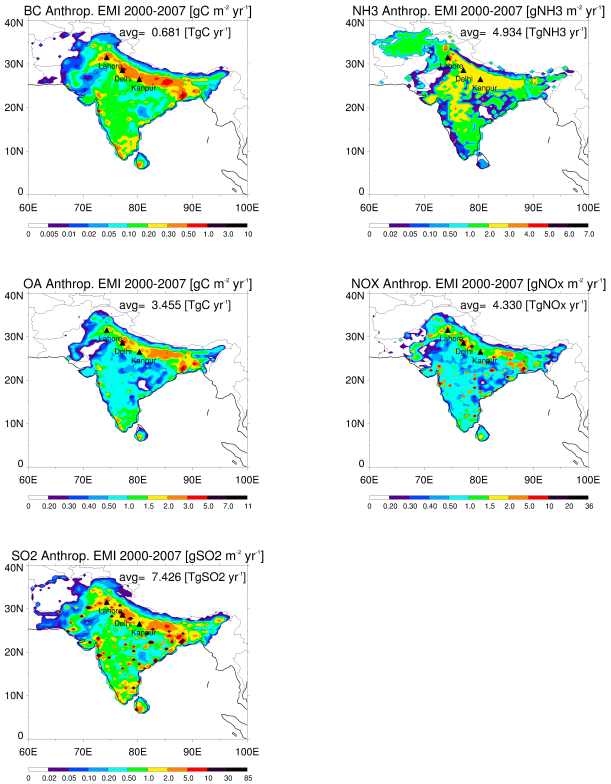

Figure 2. Spatial distribution of anthropogenic emissions of BC, OA, SO_2, NH_3 and NO_x averaged for 2000–2007 from A2-ACCMIP emission dataset (units: $g\,m^{-2}\,yr^{-1}$). The annual averaged mean emission over South Asia is shown at the upper right corner.

ACPD
14, 19095–19147, 2014

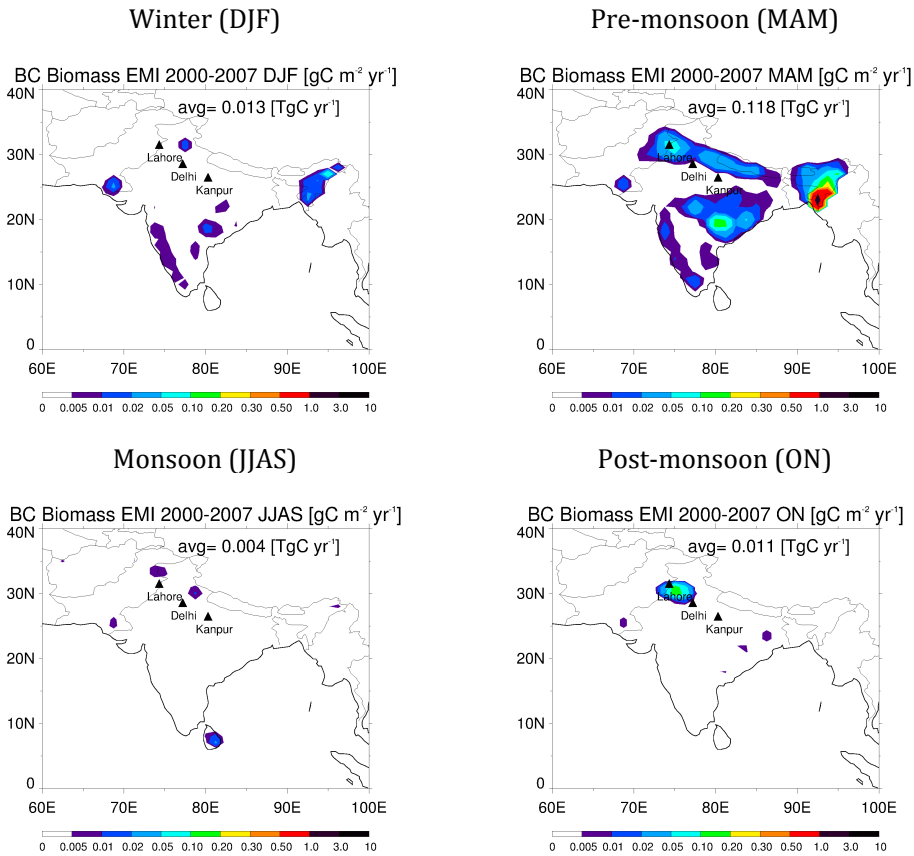

Figure 3. Spatial distribution of biomass burning emission of BC based on GFED2 for each season averaged for 2000–2007 (units: g C m^{-2} yr^{-1}). The seasonal averaged emission amount over South Asia is shown at the upper right corner. Note that the color scale is consistent with that in the Fig. 2 for BC.

ACPD
14, 19095–19147, 2014

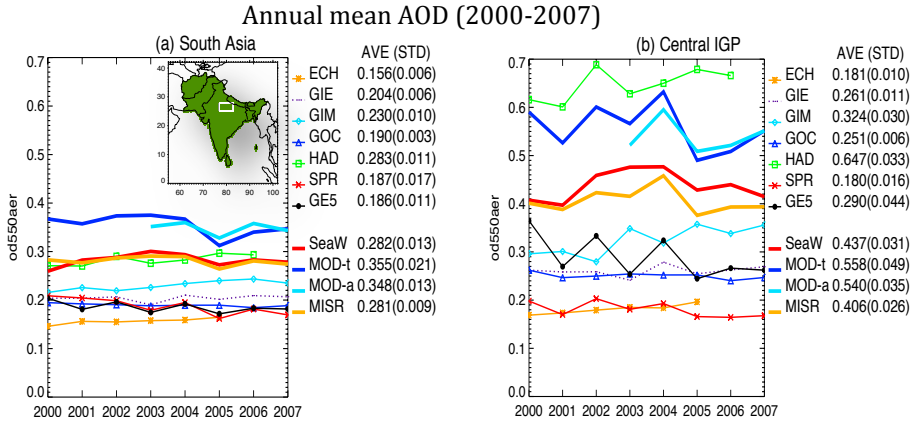

Figure 4. The annual averaged mean AOD for 2000–2007 over **(a)** South Asia (the green area in the map); **(b)** Central IGP (77–83° E; 25–28° N, the white box in that map). The thin curves with symbols represent seven models, and the thick curves represent four NASA remote sensors, with corresponding multi-year averaged annual mean AOD and the standard deviation followed.

ACPD
14, 19095–19147, 2014

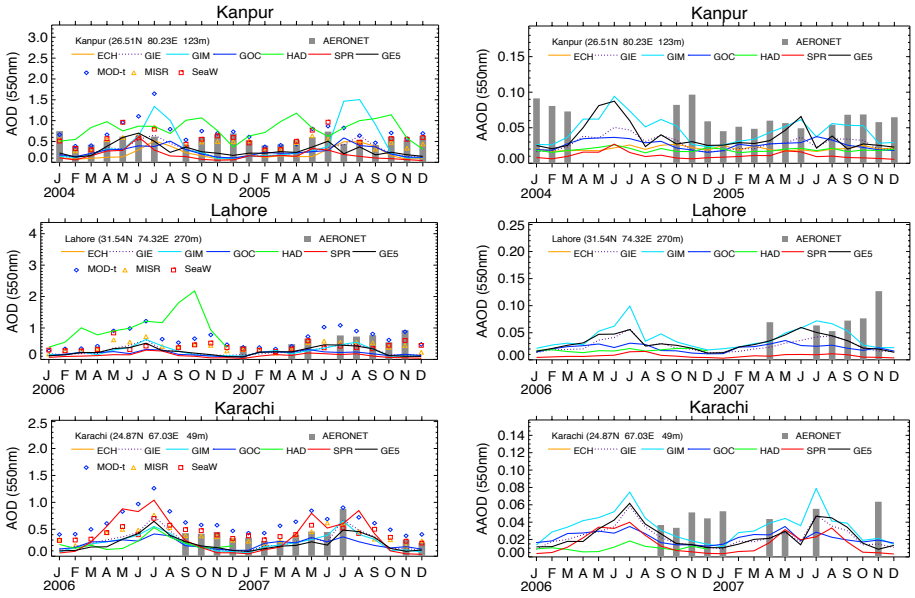

Figure 5. Monthly mean AOD (left column) and AAOD (right column) in a two-year period over 3 AERONET stations in South Asia. The gray bar represents measurement from AERONET. The thin curves represent seven models, and symbols represent three NASA remote sensors.

ACPD
14, 19095–19147, 2014

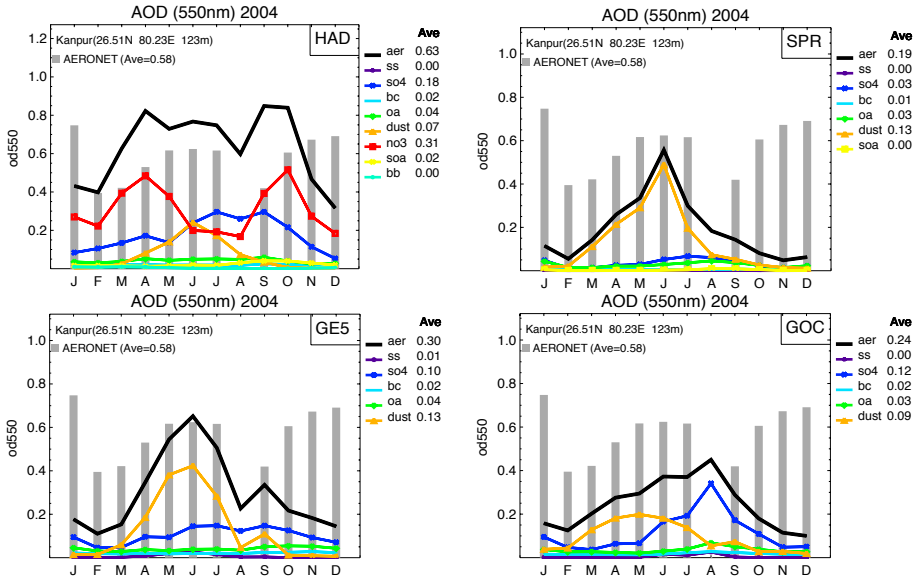

Figure 6. AOD of total aerosol (aer) and components (ss, so_4, bc, oa, dust, no_3, soa and bb) at Kanpur for 2004 in 4 models, HAD (upper left), SPR (upper right), GES (lower left) and GOC (lower right). The gray bar represents measurement from AERONET. The annual mean AOD is followed after the name of each symbol. NOTE: bc and oa represent emission from fossil fuel only and bb represents emission from biomass burning only).

ACPD
14, 19095–19147, 2014

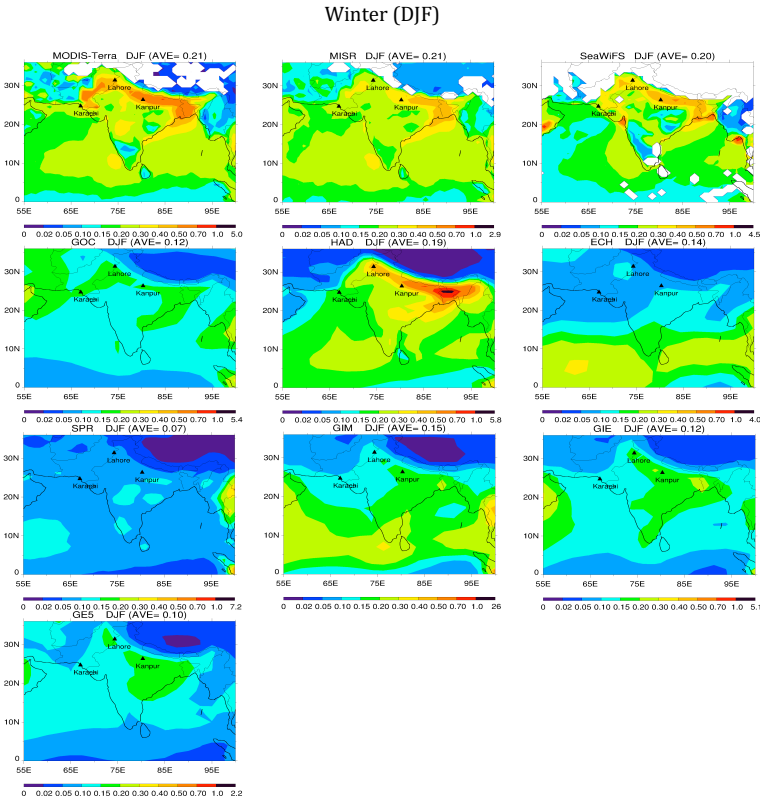

Figure 7a. Spatial distribution of AOD over South Asia in winter (DJF) averaged for 2000–2007 from three Satellite observations (the first row) and seven models (in the second row are 3 models with the anthropogenic emissions from A2-MAP and the rest are 4 models with A2-ACCMIP). The corresponding area averaged annual mean AOD is listed in each panel (domain: 0–36° N; 55° E–100° E). Three AERONET stations used in this study are labeled in the maps. Regions in white indicate insufficient sampling sizes of aerosol retrievals due to the presence of bright surface or frequent cloud cover in satellite data.

ACPD
14, 19095–19147, 2014

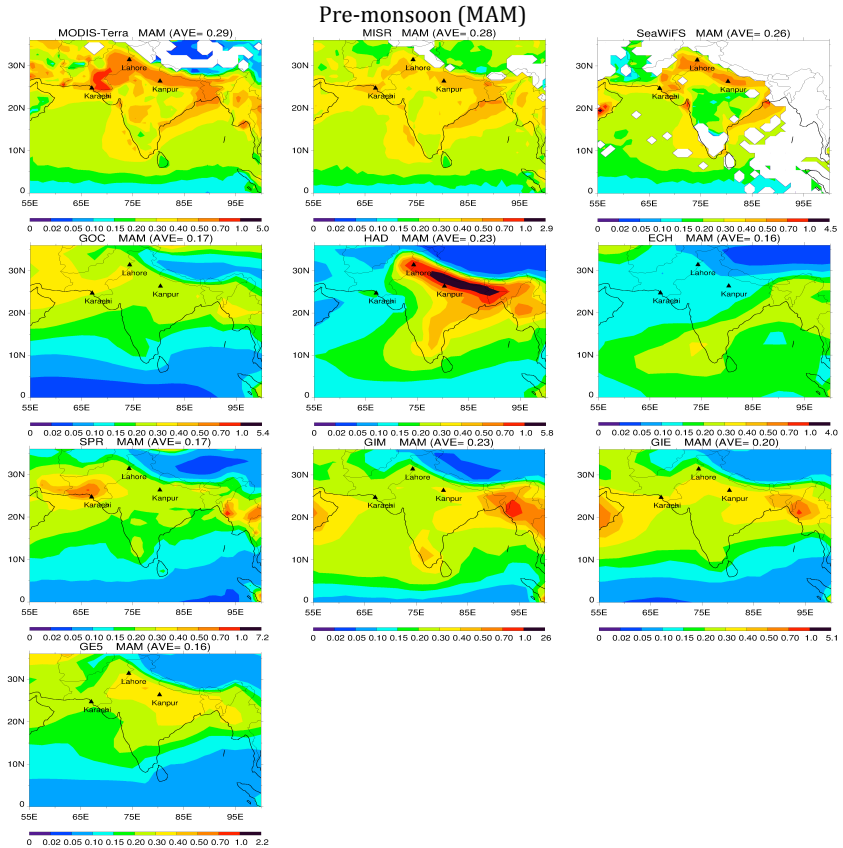

Figure 7b. Same as Fig. 7a but for pre-monsoon season (MAM).

ACPD
14, 19095–19147, 2014

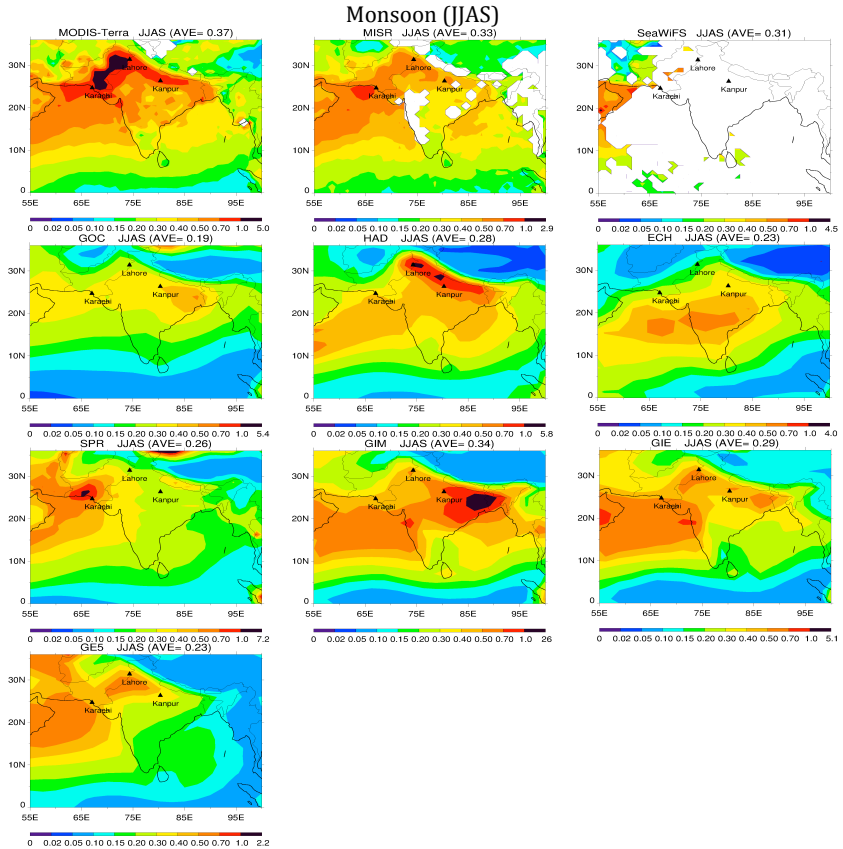

Figure 7c. Same as Fig. 7a but for monsoon season (JJAS)

ACPD
14, 19095–19147, 2014

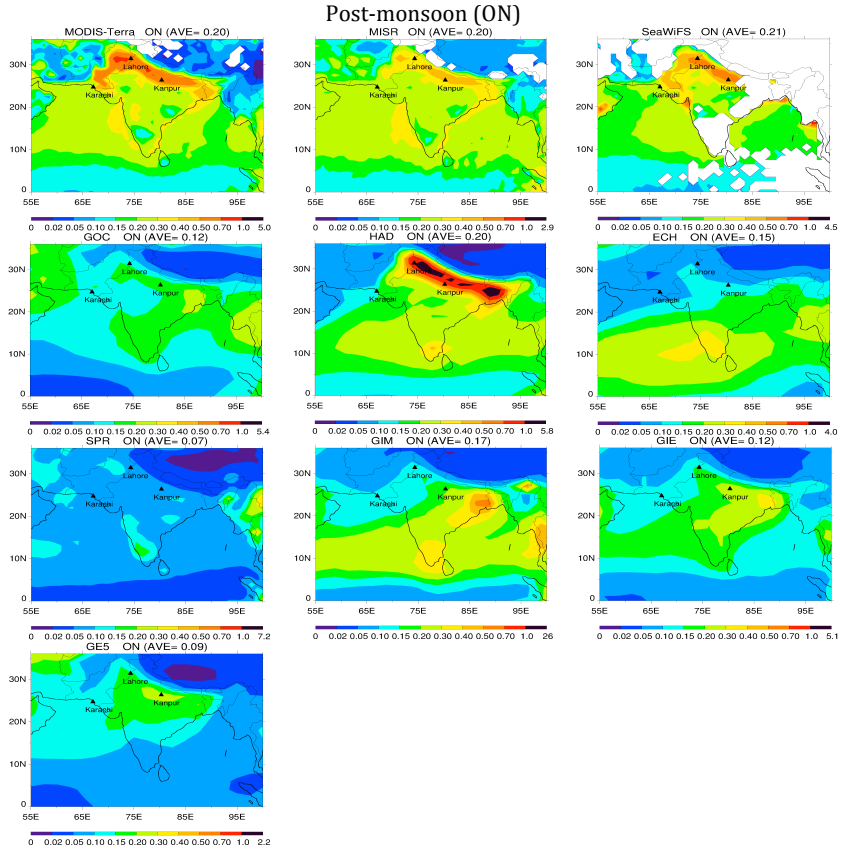

Figure 7d. Same as Fig. 7a but for post-monsoon season (ON).

ACPD
14, 19095–19147, 2014

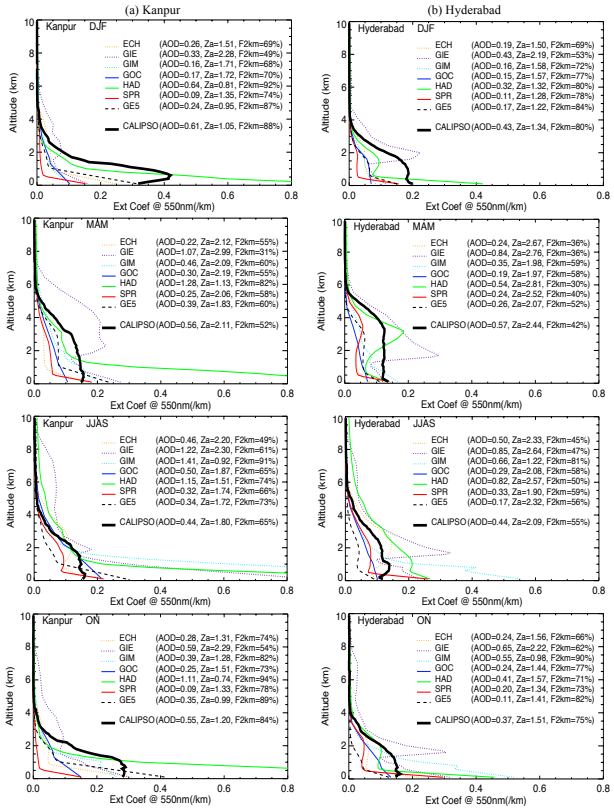

Figure 8. The seasonal variation of vertical profile of extinction coefficient (units: km^{-1}) at **(a)** Kanpur, and **(b)** Hyderabad. Units of Z_a is km. The corresponding averaged AOD, Z_a and F_{2km} are listed after each symbol name.

ACPD
14, 19095–19147, 2014

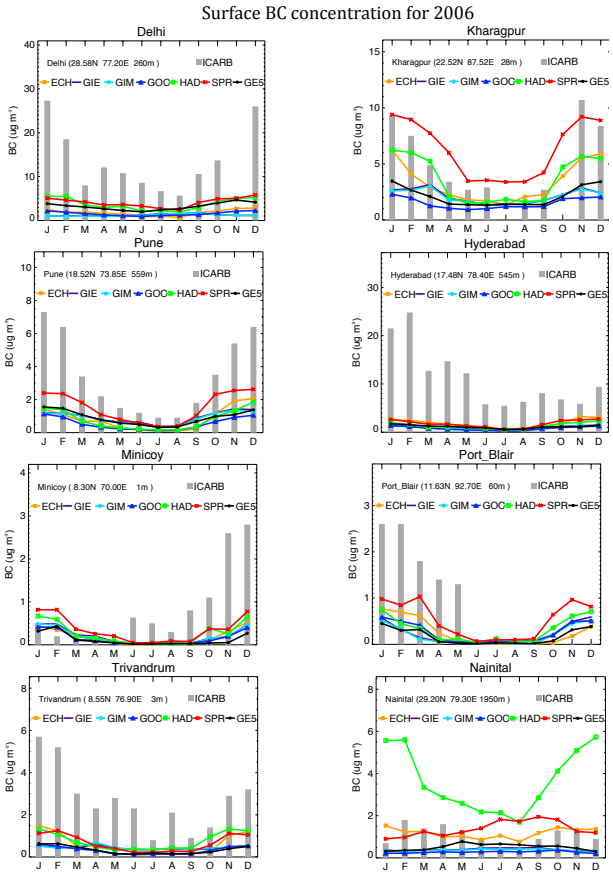

Figure 9. The comparison of seven models against observations at 8 ICARB stations in terms of monthly surface BC concentration during 2006 (units: $\mu g\,m^{-3}$).

ACPD
14, 19095–19147, 2014

A multi-model evaluation of aerosols over South Asia:

X. Pan et al.

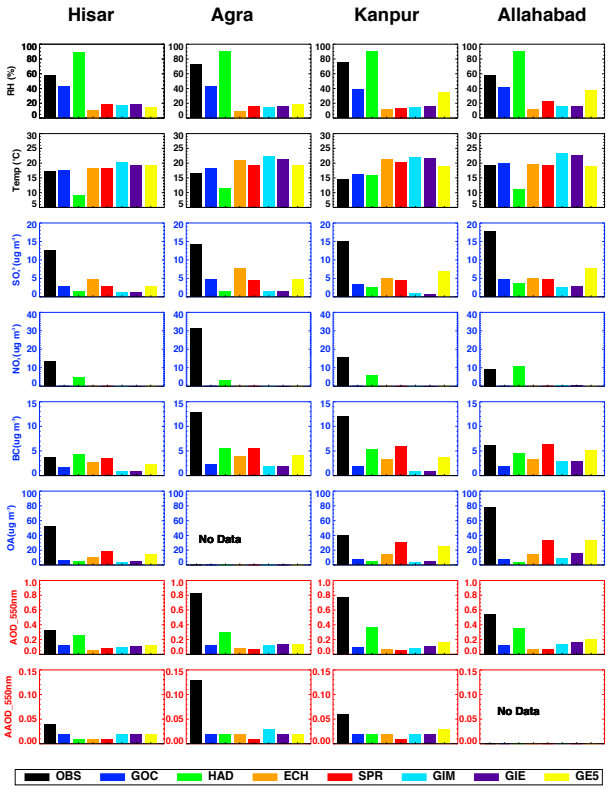

Figure 10. Comparisons of seven models against ISRO-GBP campaign measurements at 4 IGP stations (Hisar, Agra, Kanpur, Allahabad from west to east) in December 2004. The variables include two meteorological fields, surface relative humidity (1st row) and surface temperature (2nd row), four surface mass concentrations, SO_4^{2-} (3rd row), NO_3^- (4th row) with 4 models (GOC, ECH, SPR, GE5) missing this aerosol module, BC (5th row), and OA (6th row), and two columnar quantities, AOD (7th row) and AAOD (8th row) at 550 nm.

ACPD
14, 19095–19147, 2014

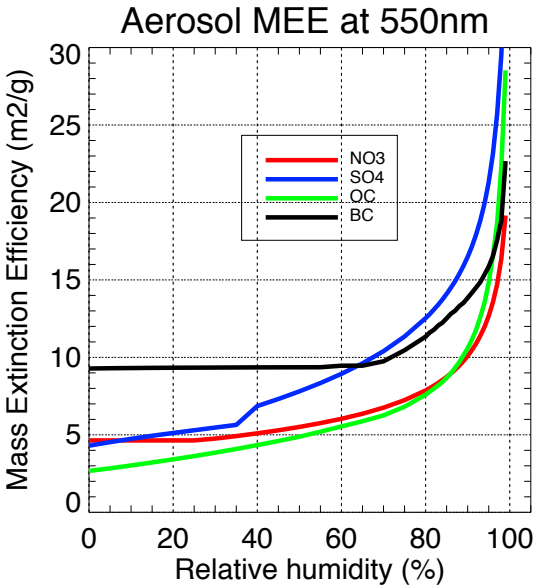

Figure 11. The mass extinction efficiency at 550 nm for individual aerosol components (units:$m^2\,g^{-1}$) as a function of relative humidity used by the models GEOS5 and GOCART.

ACPD
14, 19095–19147, 2014